Numerical optimization of Combined Heat and Power Organic Rankine Cycles – Part A: Design optimization

Emanuele Martelli*, Federico Capra, Stefano Consonni

Politecnico di Milano, Department of Energy, Via Lambruschini 4, 20156 Milano, Italy

ABSTRACT

This two-part paper proposes an approach based on state-of-the-art numerical optimization methods for simultaneously determining the most profitable design and part-load operation of Combined Heat and Power Organic Rankine Cycles. Compared to the usual design practice, the important advantages of the proposed approach are (i) to consider the part-load performance of the ORC at the design stage, (ii) to optimize not only the cycle variables, but also the main turbine design variables (number of stages, stage loads, rotational speed). In this first part (Part A), the design model and the optimization algorithm are presented and tested on a real-world test case. PGS-COM, a recently proposed hybrid derivative-free algorithm, allows to efficiently tackle the challenging non-smooth black-box problem.

1. Introduction

The utilization of renewable and low-grade heat sources for power generation has received significant attention in the past decade in view of increasing concerns over climate change and high energy prices. To this aim, closed power cycles, mainly ORC (Organic Rankine Cycles) and supercritical CO_2 cycles, have been studied, developed, and implemented at industrial scales. While supercritical CO_2 cycles are still object of research and development as well as tests [1], ORCs are nowadays widely adopted for small (100 kW) to medium scale (1–10 MW) power generation (see, e.g., the list of ORC installations by Turboden [2] and Triogen [3], two manufacturers of ORCs). Their main advantages over conventional steam cycles include higher cycle and turbine efficiencies at small scales (<1 MW) and/or low heat source temperatures (<200 °C), cheaper turbine (fewer stages and lower mechanical stress compared to a steam turbine), no blade erosion due to the adoption of dry-expansion fluids, no need of water demineralization, blow-down, and deaeration. Compared to internal combustion engines and microturbines, ORCs can use a wide variety of heat sources, including solid fuels, such as wood and straw, concentrated solar energy, geothermal heat, as well as waste heat made available by industrial processes. Hence the high popularity of ORCs.

On the other hand, the design criteria for ORCs are still object of study because of (i) the large number of available working fluids, (ii) the influence of the thermodynamic properties of the working fluid on the optimal cycle configuration, operating variables, and plant cost, (iii) the wide range of possible applications (e.g., biomass-fired combined heat and power plants, concentrated solar plants, binary geothermal plants, waste heat recovery, etc) with peculiar specifications, (iv) the ongoing research and development on turbines and heat exchangers. For these reasons, more than four hundred papers have been published so far on the topic of ORC optimization, and most of them in the last four years [4]. However, only a few of them use rigorous mathematical models of the plant and apply numerical optimization algorithms. In the next subsection we briefly summarize the main works which use numerical optimization algorithms to determine the best ORC design.

1.1. Previous works on the optimization of ORC design

Dai et al. [5] develop a thermodynamic model of a waste heat recovery ORC which, for fixed cycle variables, determines the performance of the cycle. The exergy efficiency of the cycle is maximized with a "black-box" approach (see for further details [6]): the cycle model is executed by the optimization algorithm as a "black-

* Corresponding author. Tel.: +39 0523356813; fax: +39 0523623097.
E-*mail address:* emanuele.martelli@polimi.it (E. Martelli).

Published Journal Article available at: http://dx.doi.org/10.1016/j.energy.2015.06.111

box" function. The optimization algorithm varies the design variables looking for the minimum of a selected objective function, and, for each sampled solution, an ad hoc routine solves the model to evaluate the cycle performance. In Dai et al. [5] the cycle model is solved with an ad hoc iterative routine written by the authors in Fortran, while the optimization problem is tackled with an undefined Genetic Algorithm. The decision variables are only two, the turbine inlet temperature and pressure. The optimization of the cycle variables is repeated for ten different working fluids. Papadopoulos et al. [7] present an approach for the optimal selection of working fluids for ORCs based on a multi-objective Computer Aided Molecular Design technique. The designed molecules are Pareto optimal with respect to a set relevant physical properties such as density, heat of vaporization and liquid heat capacity. The actual performance of the optimized fluids is evaluated with a simplified thermo-economic model of the ORC. Rashidi et al. [8] build the thermodynamic model of regenerative ORCs in EES (Engineering Equation Solver, a commercial software package used for solution of systems of non-linear equations, [9]) and use the model results to train a neural network. Then, an artificial bees colony algorithm optimizes the regeneration pressures referring to the trained neural network to evaluate the performance indexes of the cycle. Wang et al. [10] propose a Matlab model of a low temperature waste heat recovery ORC which includes thermodynamic, heat transfer and economic relations. A set of thirteen working fluids is defined, and for each of them the main four design variables (pressures of evaporation and condensation pressures, and velocities of working fluid and cooling water in the heat exchangers) are optimized with a black-box approach: the cycle simulation code is executed as a black-box function by a Simulated Annealing algorithm (details are not specified). Wang et al. [11] adopt a similar black-box approach to optimize an ORC for low grade waste heat recovery. Their ther-modynamic model, coded in Matlab, includes a detailed heat transfer calculation of the heat exchangers aimed at determining the required heat transfer area. Assuming that the overall capital cost of ORC system is dominated by the cost of the heat exchanger area, the authors consider the ratio net power output/heat transfer area as objective function, and adopt a Genetic Algorithm (since not specified, it is supposed to be algorithm of Conn et al. [12] which is available in the Matlab Global Optimization toolbox [13]) to opti-mize the turbine inlet pressure and temperature, and the temper-ature differences of the heat recovery generator (at pinch and approach points). Later, in Ref. [14], the model is improved by adding an economic model, and including the condenser temper-ature difference into the set of optimization variables. The trade-off between maximum exergy efficiency and minimum capital cost is evaluated by setting a multi-objective optimization problem and tackling it with the NSGA-II algorithm [15] which is implemented in the Matlab Global Optimization toolbox [13]. Xi et al. [16] maximize the exergy efficiency of regenerative ORCs for low temperature waste heat recovery. It is worth noting that regenerators are mixers: before entering the heat recovery generator, the liquid stream is mixed with the vapor extracted from the turbine. Following a black-box strategy, the cycle simulation is solved by a code implemented by the authors, while the decision variables (namely, turbine inlet temperature and pressure, and the fraction of flow rate to the regenerators) are optimized with a genetic algorithm combining different improved evolution operators. Pierobon et al. [17] propose a multi-objective optimization approach for the design of heat recovery ORCs for offshore platforms (where cycle weight and size matter). The multi-objective genetic algorithm NSGA-II of [15] controls a Matlab routine (the black-box) which solves the cycle, design the heat exchangers, and works out the overall efficiency, net present value and volume. The decision var-iables of the GA are: working fluid type, condenser outlet temperature, turbine inlet pressure, superheating temperature difference, pinch point temperature differences of condenser, regenerator, economizer and evaporator, and fluid velocities in each heat exchanger. The black-box routine contains not only the cycle solver but also an inner optimization procedure which determines the heat exchanger geometry for fixed fluid velocities with the Nelder-Mead method [18]. A similar black-box approach with just a simplified cycle model is used by Andreasen et al. [19] to optimize the mixture composition and cycle variables of ORCs for low grade heat recovery.

Lecompte et al. [20] are the first ones to propose a strategy for optimizing the thermo-economic design of ORCs which takes into account of the part-load performance of the cycle over the expected year of operation. Their study is focused on a ORC recovering waste heat from an internal combustion engine with time-dependent load. They want to determine the best cycle design for the ex-pected yearly scheduling of the engine and ambient temperature (affecting condenser performance). Hence, they define a sampling grid of nominal design conditions (ambient temperature and thermal power provided by the engine), and for each point they determine (1) the design variables which minimize the specific (nominal) investment cost with the Nelder-Mead method [18], (2) the part-load map of the optimized cycle expressing the net power output as a function of the ambient temperature and engine load (the part-load operation is solved with a cycle simulation code built in Matlab and linked to the Golden Section Search algorithm to optimize the mass flow rate of cooling air), (3) the behavior of the optimized cycle over the year and the actual annual specific cost. Once the actual annual specific cost of each grid point is computed, a polynomial model is regressed and used to determine the optimal design condition (ambient temperature and thermal power provided by the engine) and associated design variables. Pierobon et al.[21] improve the design optimization model and algorithm of [17] for heat recovery ORCs, and combine it with a dynamic model in order to select the most flexible solutions. First the Pareto-optimal solutions with respect to efficiency and volume are found with the steady-state model, then their dynamic performance is evaluated with Modelica [22]. Maraver et al. [23] tackle the thermodynamic optimization of ORCs for waste heat recovery systems, CHP (combined heat and power) plants, and binary geothermal power plants. After identifying the most common fluids used in commercial ORC units, they build a basic thermodynamic model of the cycle and optimize the exergy efficiency of the cycles by varying the inlet turbine pressure and superheat temperature with the direct-search algorithm DIRECT (DIviding RECTangles, [24]).

Walraven et al. [25] develop a model to simultaneously optimize the cycle variables and the design variables of the heat exchangers. The cycle is modeled with the energy and mass balance equations of the pieces of equipment (pump, turbine, heat exchangers, mixers, splitters), while the heat transfer coefficients and pressure drops of each heat exchanger are computed with the Bell—Dela-ware method. An equation oriented approach (in which optimiza-tion and model solution are simultaneous because the model equations are included in the optimization problem as constraints, see Ref. [26]) is used to optimize the turbine inlet temperature, the evaporation temperature, the fluid mass flow rate, the condenser temperature, the regenerator minimum temperature difference, and the geometrical variables of the heat exchangers. The objective function is the exergy efficiency of the plant which can be achieved for a given total heat exchanger area. The gradient-based WORHP algorithm of Buskens & Wassel [27] is applied, and gradients are calculated with automatic differentiation. In Ref. [28] the authors add the models of the axial turbine and air-cooled condenser.

Larsen et al. [29] tackle the optimization of heat recovery power cycles (including ORCs) for large ship engines adopting a black-box

approach: a Genetic Algorithm optimizes a few design variables (working fluid, evaporation pressure, superheater approach temperature) executing for each trial solution a Matlab routine which simulates the ship engine and computes the fluid mass flow rates and the cycle performance indexes.

Toffolo et al. [30] optimize the design of ORCs for binary geothermal power plants. The cycle configuration (heat exchanger network) and variables (working fluid mass flow rate, evaporation pressure, condensation pressure and superheating degree) are optimized for maximum efficiency with the HEATSEP method [31] for two working fluids (isobutene and R134a). The Sequential Quadratic Programming algorithm of the Matlab Optimization Toolbox [32] optimizes the intensive cycle variables while the working fluid flow rate is adjusted within the problem table algorithm which handles the heat integration between hot and cold streams. Then the levelized cost of electricity is evaluated for the maximum efficiency solution and a set of neighboring sub-optimal solutions with a validated economic model. For each solution, the electricity generated over the operating year is assessed with yearly simulations of the plant operation with the off-design model pre-sented in Ref. [33] so as to take into account of ambient temperature variations. The best solution in terms of minimum levelized cost of electricity, which does not coincide with the one of maximum efficiency, is picked up from the set of neighboring solutions.

1.2. Contribution of this work

It is worth noting that, even though the expansion efficiency and capital cost of the turbine have a large effect on the final perfor-mance figures of the cycle, none of the above mentioned approaches optimizes the turbine design variables (e.g., for an axial or radial turbine: number of stages, rotational speed, loads of each stage, maximum peripheral velocity, etc) together with those of the cycle. To the best of our knowledge, only Astolfi et al. [34] have recently proposed a model for optimizing the design of binary geothermal power cycles which includes a detailed turbine model. However, it is important to note that in their work the turbine design is not numerically optimized. For each cycle design, the turbine is designed on the basis of sound engineering criteria which lead to a limited number of stages with close-to-optimal expansion efficiency. The most important design assumptions are (1) the number of stages is computed on the basis of the maximum allowed stage volume flow ratio and maximum allowed stage isentropic enthalpy drop, (2) if multiple stages are necessary, stage loads are adjusted so as to have equal volume flow ratio or enthalpy drop (depending on which limit is violated), (3) only the isentropic efficiency of the first and last stages are computed, and the overall turbine isentropic efficiency is assumed to be the average value so as to save computational time, (4) the rotational speed is set equal to the optimal value for the last stage. The stage isentropic efficiency is evaluated on the basis of the results obtained by of Macchi & Perdichizzi [35] for axial-flow turbine stages operating with unconventional fluids. The turbine cost is expressed as a function of the power output, size parameter (see the definition in Subsection 4.1.2) and number of stages with a correlation developed by the authors.

In Part A of this two-part paper, we propose a thermo-economic model and an effective algorithm for the simultaneous optimization of the cycle variables, turbine design, and heat exchanger areas. The study is focused on biomass-fired CHP ORCs and the optimi-zation involves the design variables of the cycle (evaporation and condensation pressures, superheating degree), heat exchangers (pinch point temperature differences of each heat exchanger), and turbine (number of stages, rotational speed and load distribution over the stages). The above described design assumptions (1–4) made by Astolfi et al. [34] are removed, and the main turbine design variables are numerically optimized together with the main design variables of the plant following a black-box strategy. The system configuration and the most important optimization variables are identified in Section 2 on the basis of thermodynamic considerations. The overall optimization methodology is described in Section 3, the thermo-economic model is detailed in Section 4, and the optimization algorithm is described in Section 5. In Section 6 the design optimization approach is tested on a real-world design problem.

In Part B of this work [36], a novel off-design operation optimization model is proposed, and it is combined with design optimization model (presented in Part A) to accurately evaluate the impact of the part-load behavior on the design of the plant. Indeed, due to their relatively poor efficiency, biomass-fired ORCs for CHP applications are typically controlled to follow the time profile of the heat demand. For this reason, CHP ORC units are asked to operate at part-loads for most of the time, and their optimal size and design must be evaluated taking into account of the heat demand duration curve and their off-design performance.

2. Thermodynamic analysis

A biomass-fired CHP ORC plant is typically made of a biomass-fired boiler, a loop of hot oil transferring heat from the boiler to the cycle, a heat exchanger in which the working fluid is economized, evaporated and superheated, a turbine, a regenerator, and a condenser which supplies thermal power to a heat user (e.g., a building or a district heating network) through a water loop. A schematic representation is reported in Fig. 1.

In order to determine the design variables which need to be optimized, the thermodynamics of the system is thoroughly analyzed.

For a Rankine cycle (using any type of working fluid) with fired boiler, the net electric efficiency of the plant η_{EL},

$$\eta_{EL} = \frac{\dot{W}_{EL}}{\dot{m}_{FUEL} \cdot LHV_{FUEL}}, \tag{1}$$

can be expressed as the product of the boiler thermal efficiency η_B,

$$\eta_B = \frac{\dot{Q}_C}{\dot{m}_{FUEL} \cdot LHV_{FUEL}}, \tag{2}$$

and the net electric efficiency of the cycle η_C,

$$\eta_C = \frac{\dot{W}_{EL}}{\dot{Q}_C}, \tag{3}$$

as shown in Eq. (4),

$$\eta_{EL} = \eta_B \eta_C. \tag{4}$$

In Eqs. (1)–(4), $\dot{W}_{EL}$ denotes the net electric power of the plant, $\dot{m}_{FUEL}$ the fuel mass flow rate, LHV_{FUEL} the fuel lower heating value, and $\dot{Q}_C$ the thermal power transferred from the boiler to the cycle.

According to the indirect method for the calculation of the boiler efficiency, η_B can be maximized by limiting the heat losses from the boiler casing, setting the proper percent excess air (defined as the mass flow rate of excess air and the stoichiometric air mass flow rate) for the given types of fuel and boiler (typically in the range 50–200% for wood chips [37]), and designing the boiler for the lowest allowed gas stack temperature. It is important to note that, if the boiler has an air preheater, the gas stack temperature does not

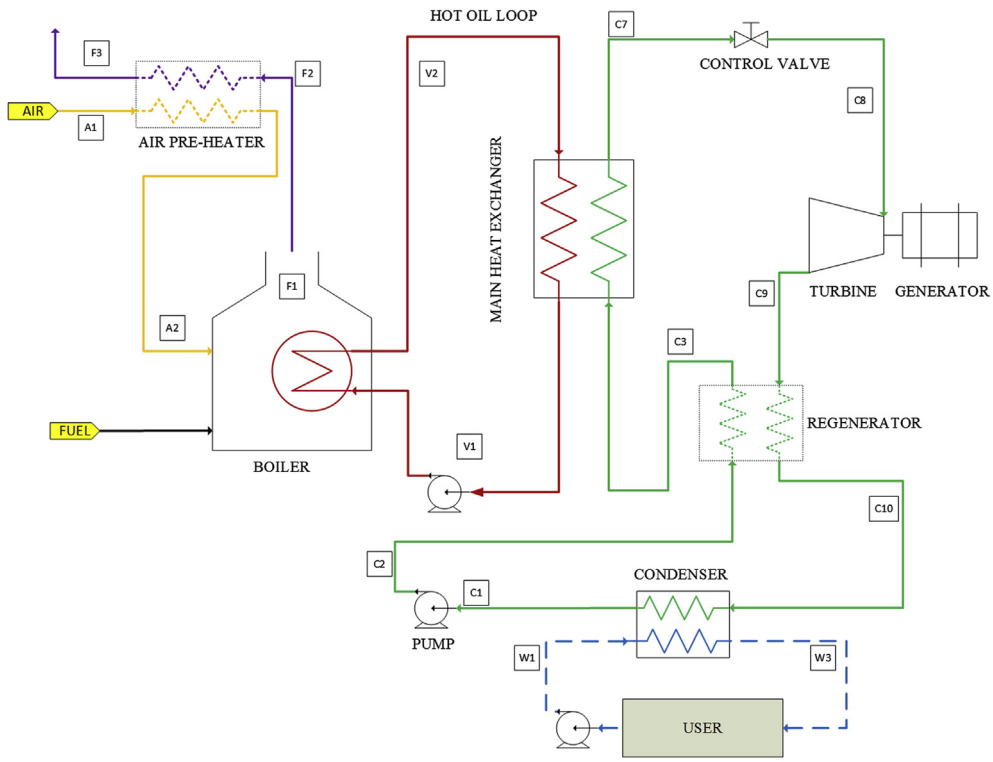

Fig. 1. Schematic representation of a biomass-fired ORC for CHP applications.

depend on the design of the Rankine cycle because in any case flue gases can be cooled down to close-to-ambient temperature by the air. Hence, it is possible to independently maximize η_B and η_C. In practice, the stack temperature is set at the minimum value necessary to have the desired stack draught, and/or to avoid condensation of acid species and water. It is worth noting that, if the boiler does not have the air preheater, the design of the thermodynamic cycle can have influence on η_B as the stack temperature T_{F2} must be greater than the oil return temperature T_{V1} which, in turn, is greater than the regenerator exit temperature T_{C3} (see Fig. 1). In that case adopting a heavy regeneration degree (high T_{C3}) penalizes the boiler efficiency. For this reason the cycle variables and the boiler stack temperature need to be optimized at once looking for the maximum product of η_B and η_C (similarly to what is done for heat recovery cycles in Ref. [38]).

As far as the cycle net electric efficiency η_C is concerned, the following variables must be considered:

- working fluid,
- boiler pressure,
- condenser pressure,
- superheating degree.

While the thermodynamic effects of boiler and condenser pressures on η_C are well-known, the influence of the superheating degree on cycle efficiency depends on the type of working fluid and on the effectiveness of the regenerator.

2.1. Rankine cycles with wet-expansion fluids

For fixed boiler and condenser pressures, if the selected working fluid is of the "wet-expansion" type (i.e., with a negative slope of the vapor saturation curve in the temperature – entropy diagram [39] like water and ammonia), the net cycle efficiency increases with the superheating degree. Besides superheating (as well as reheating), the net cycle efficiency can be increased by adding regeneration. Since the expansion line typically falls within the saturation curve, regeneration must be implemented by heating up the pressurized liquid with a cascade of vapor streams extracted from the turbine at intermediate pressures. If extraction pressures and flow rates are optimized, regeneration has a positive effect on the net cycle efficiency.

2.2. Rankine cycles with dry-expansion fluids

Concerning "dry-expansion" working fluids (i.e., with a positive slope of the vapor saturation curve like toluene and MDM (C8H24O2Si3 octamethyltrisiloxane), the net cycle efficiency may even decrease with the superheating degree. If the cycle is not regenerative and the slope of the vapor saturation curve is highly positive, the net cycle efficiency decreases with the superheating degree, as found by Refs. [40], [41]. Fig. 2 plots the net cycle efficiency (defined as the net power output divided by the thermal power input) of an ideal subcritical Rankine cycle without regeneration as a function of the superheating degree (difference between the superheat temperature and the evaporation temperature) for MDM, toluene and water. In order to have a fair comparison, the plot assumes the same evaporation and condenser temperatures (i.e., 290 and 80 °C respectively) for all fluids.

Since for toluene and MDM the turbine outlet condition is outside the saturation curve (see Fig. 3(A) and (B)), the higher is the superheating degree and the higher is the average temperature of the heat rejection phase. The limited divergence of the boiler and condenser isobaric curves in the *T-s* (temperature – entropy) diagram (see Fig. 3(A) and (B)) makes the positive effect (increase of the average heat input temperature) smaller than the negative one (rise of the average heat rejection temperature), and this leads to a decrease of the cycle efficiency. It is worth noting that MDM has a

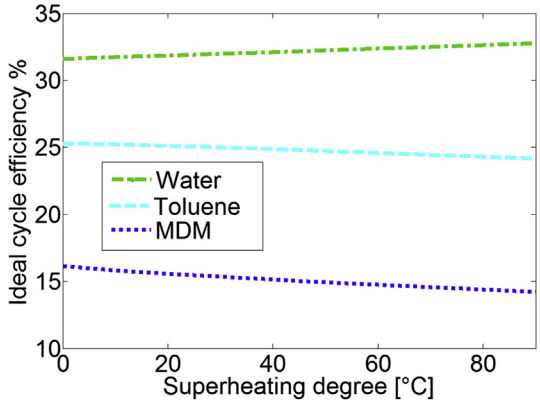

Fig. 2. Net cycle efficiency of an ideal Rankine cycle without regeneration as a function of the superheating degree for water, toluene and MDM.

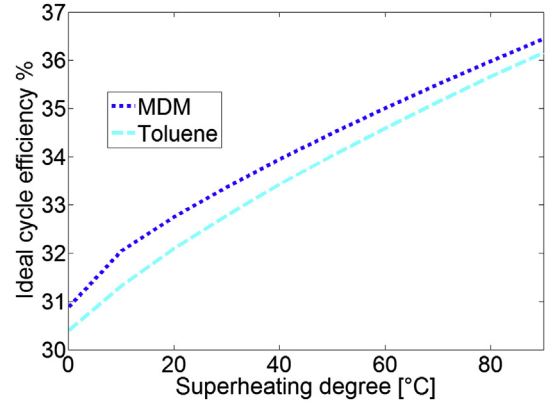

Fig. 4. Net cycle efficiency of an ideal Rankine cycle with ideal regeneration (regenerator effectiveness equal to one) as a function of the superheating degree for toluene and MDM.

lower net cycle efficiency than toluene over the whole range of superheating degree. This difference can be explained looking at the *T*-*s* (temperature – entropy) diagrams of the two cycles. The MDM cycle has (i) a lower average heat input temperature due to the lower ratio between the heat required for evaporation and the heat required for liquid preheating (about 5.4% for MDM and 33.8% for toluene), (ii) a higher average heat rejection temperature due to the small temperature drop across the expansion. As well explained in Refs. [42], effect (i) is mainly due the higher molecular mass of the fluid (236.5 kg/kmol, and toluene 92.3 kg/kmol), while effect (ii) depends on the slope of the vapor saturation curve which in turns depends on the molecular complexity of the fluid. Indeed, water reaches the highest efficiency because of the high evaporation enthalpy (thanks to its small molecular mass) and heat rejection transformation at the minimum temperature (due to its simple molecular structure which corresponds to a negative slope of the saturated vapor curve). Moreover, the large divergence of the boiler and condenser isobaric curves makes superheating advantageous for the net cycle efficiency.

However, the results may significantly change if superheating is combined with regeneration. With dry-expansion fluids, since the turbine outlet temperature is sufficiently higher than the pump outlet temperature, regeneration can be easily implemented by adding a heat exchanger at the turbine outlet to recover the heat released in the vapor de-superheating phase (as represented in Fig. 1). This decreases the heat required by the liquid preheating step, and then increases the cycle efficiency. Besides, if the regen-erator has a good effectiveness and contained pressure drops, regeneration makes superheating beneficial to cycle efficiency. In Fig. 4 the net cycle efficiency of an ideal Rankine cycle with ideal regenerator (no pressure drops and effectiveness equal to one, i.e., capable of cooling the hot vapor stream up to the liquid inlet temperature) is plotted as a function of the superheating degree for MDM and toluene. For both fluids, the net cycle efficiency increases with the superheating degree because, thanks to the regenerator, superheating increases the average heat input temperature without increasing the average heat rejection temperature. Hence, it cannot be generally stated that superheating is detrimental for the ORCs with dry-expansion fluids. Its effect on cycle efficiency depends on the effectiveness of the regenerator. Fig. 4 also shows that, if the cycle is regenerative, MDM performs better than toluene, reversing the results obtained in Fig. 2 without regenerator.

2.3. Maximum temperature and cogeneration

When optimizing the thermodynamic performance of a biomass-fired ORC, although combustion makes available very hot flue gases (even above 900 °C) and commercially available materials for boiler applications can stand temperatures up to 550–600 °C without major concerns [38], it is necessary to set a rather low upper bound on the maximum cycle temperature. Indeed, the working fluid temperature cannot be increased above a certain limit set by the thermal stability of its molecules (e.g., about 400 °C for methylsiloxanes and toluene, 300–350 °C for linear hydrocarbons [42]) or the maximum operative temperature of the hot oil loop (about 300 °C [2]). Thus, for the given maximum cycle temperature, the best combination of working fluid, evaporation temperature, superheating degree and regenerator design must be carefully evaluated through numerical optimization.

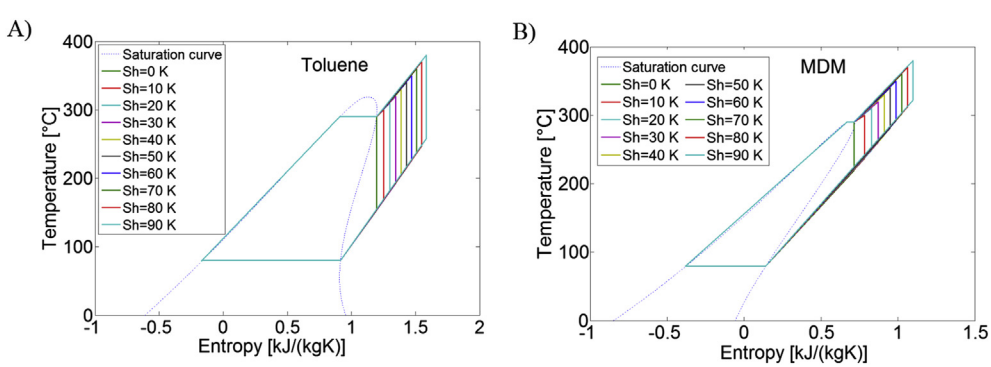

Fig. 3. $T-s$ (temperature – entropy) diagrams of the ideal Rankine cycle for superheating degree ranging from 0 °C to 90 °C with toluene ($T-s$ diagram A) MDM ($T-s$ diagram B) as working fluid.

When studying a CHP plant, not only the plant net electric efficiency, but also the plant thermal efficiency η_{TH} (defined as the thermal power supplied to the heat user and the fuel power input) matters. The plant is sized to match the demand of thermal power of the heat user, and the condensation temperature is set according to the user's temperature requirement. Concerning η_{TH} and its relation with the cycle variables, it is sufficient to note that η_{TH} can be expressed as the product of the boiler efficiency η_B and the cycle thermal efficiency η_Q,

$$\eta_{TH} = \eta_B \eta_Q, \tag{5}$$

where η_Q is defined as the ratio between the thermal power supplied to the heat user $\dot{Q}_{USER}$ and that entering the cycle $\dot{Q}_C$,

$$\eta_C = \frac{Q_{USER}}{\dot{Q}_C}. \tag{6}$$

If the mechanical, electrical and heat losses of equipment units are neglected and all the condensation heat is provided to the heat user, the first principle of thermodynamics (i.e., the energy balance equation of the cycle) guarantees that

$$\eta_Q \cong 1 - \eta_C. \tag{7}$$

Thus, plant thermal efficiency η_{TH} can be expressed as in the following equation,

$$\eta_{TH} \cong \eta_B (1 - \eta_C). \tag{8}$$

Eq. (8) clearly shows that the plant net electric efficiency and the plant thermal efficiency are conflicting objectives. From a thermodynamic point of view, when dealing with cogeneration systems, the proper balance between η_{TH} and η_{EL} is determined by introducing the exergy efficiency (or second law efficiency) η_{II}, defined as

$$\eta_{II} = \frac{\dot{W}_{EL} + \dot{Q}_{USER}\left(1 - \frac{T_0}{T_{USER}}\right)}{\dot{m}_{FUEL} \cdot EX_{FUEL}}, \tag{9}$$

where T_0 is the dead state (or ambient) temperature, T_{USER} is the temperature level required by the heat user, and EX_{FUEL} is the fuel chemical exergy. Such objective function is considered for instance by Ref. [23]. However, when dealing with a commercial plant, the best trade-off between η_{TH} and η_{EL} must be determined with an economic optimization. For instance, if the electricity price is very low, it is not advantageous to build a CHP plant and the optimal plant design turns out to be a boiler (corresponding to the solution with maximum plant thermal efficiency, since $\eta_C = 0$ and $\eta_{TH} \cong \eta_B$). Viceversa, if the electricity price is significantly high, it is advantageous to design a plant for the maximum electric efficiency, and even oversize the plant with respect to the heat demand (wasting part of the condensation heat).

3. Problem statement and optimization approach

The thermodynamic analysis reported above indicates the need of numerical optimization methods to determine the cycle variables which maximize the thermodynamic efficiency of an ideal cycle. Optimizing the design a real ORC plant is even more challenging as (i) a detailed turbine model is necessary to assess the actual expansion efficiency, (ii) the main design variables of turbine and heat exchangers must be included in the optimization, (iii) an economic model is needed to work out the effects of the decision variables on profitability.

The plant model considered in this work is detailed in Fig. 5. Since this study is focused on relatively large units (thermal power to the heat user above 5 MW), the boiler is assumed to have an air preheater so as to maximize the heat recovery from the flue gases without penalizing the cycle efficiency. The turbine is assumed to be axial with one or multiple stages, and a single shaft. The heat exchanger between hot oil and working fluid is conceptually divided into three sections, the economizer, the evaporator and the superheater, in order to take into account of their different heat transfer properties. Similarly, the condenser is split into a vapor desuperheating section and the two-phase condensation section.

The optimization problem tackled in this work can be stated as follows.

Given

- the plant configuration of Fig. 5,
- the elemental composition, moisture content, and lower heating value of fuel,
- the nominal (full-load) demand of thermal power,
- the expected number of full-load equivalent hours per year of the heat demand (or the total amount of heat required by the user over one year),
- the inlet and outlet water temperatures required by the heat user,
- the economic data related to the operation of the plant (i.e., cost of fuel, price of electricity, CO_2 credits, etc)
- the financial assumptions of the investment (for example grouped into the levelized capital charge rate [43]), determine the plant design which maximizes the annual profit.

The design variables optimized in this work are listed below:

- Evaporation pressure, p_{EVA}
- Condensation pressure, p_{COND}
- Superheating degree, ΔT_{SH}
- The pinch point temperature difference in the regenerator $\Delta T_{PP,REG}$ (which indirectly determines the heat transfer area of the regenerator)
- Pinch point temperature difference of the main heat exchanger $\Delta T_{PP,MHE}$ (which determines the heat transfer area)
- Turbine rotational speed, ω
- Number of turbine stages, N_{ST}
- Load (or equivalently the pressure ratio β) of each turbine stage, $\beta_i \ \forall \ i \in \{1, \ 2, \ \ldots, \ N_{ST}\}$

It is worth noting that the heat transfer area of both superheater and regenerator are indirectly optimized by setting the pinch point temperature difference. Besides, if they have a negative effect on the cycle efficiency or cost, they can be automatically eliminated by the optimization algorithm by properly setting their temperature differences. If superheating is not advantageous, the optimizer will set ΔT_{SH} to its lower bound (1 K, as discussed in Section 6). If the regenerator is not advantageous, the optimizer can set $\Delta T_{PP,REG}$ to a value equal or greater than $T_{C9}-T_{C2}$. In this way, the regenerator heat duty, area, cost and pressure drops are set to zero.

On the other hand, aside from the possibility of automatically removing the regenerator and the superheater, it is important to note that the cycle layout is fixed and not systematically optimized. Indeed such a structural optimization would require process synthesis methods (i.e., superstructures [26]) as well as integer (Boolean) variables, and the use of Mixed Integer NonLinear Programming algorithms (MINLP). Tackling such problem is out of the scope of this work.

As far as the number of turbine stages is concerned, its direct optimization is avoided by properly building the turbine design

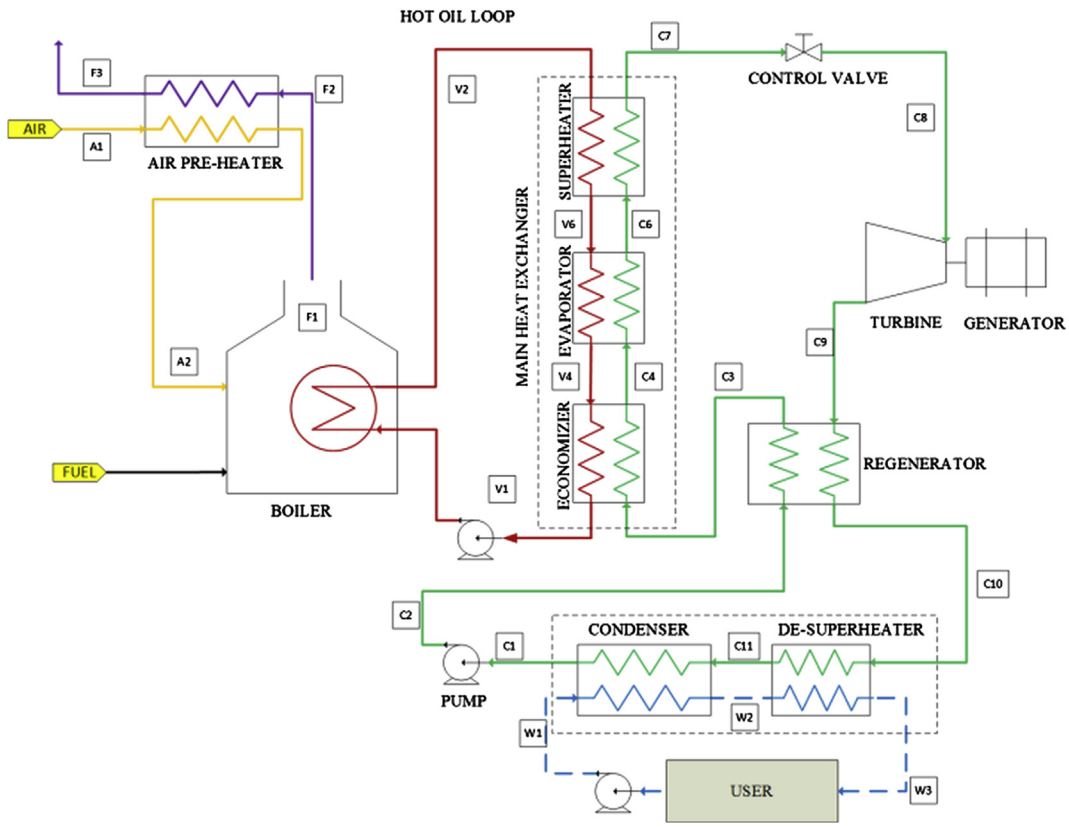

Fig. 5. Detailed scheme of the plant model adopted in this work.

model (see Subsection 4.1.2). Indeed, the turbine design algorithm computes the number of stages corresponding to the given stage loads. On one hand this approach avoids considering discrete variables, but on the other hand it causes objective function discontinuities when the turbine design algorithm changes the number of stages (see Section 5).

The selection of the optimal working fluid is not addressed by numerical optimization. Indeed, it is not correct to optimize categorical variables (i.e., discrete variables having no natural ordering in the decision space) with nonlinear programming algorithms (whether NLP or MINLP) as their progress and convergence to an optimum rely on the existence of a distance measure between explored solutions [44]. For instance, associating each fluid type to a discrete variable and using a genetic algorithm to optimize the fluid selection variable may overlook the optimum solution as the optimization algorithm implicitly assumes the existence of a natural ordering of the fluids. For this reason, in order to determine the best working fluid, we first define a set of promising working fluids, and then repeat the design optimization for each of them.

As previously mentioned, the design optimization problem is tackled with a black-box approach (see Fig. 6): a derivative-free optimization algorithm explores the solution space of independent design variables (pressures of evaporation and condensation, pinch point temperature differences of MHE and condenser, superheating degree, turbine rotational speed, maximum pressure ratios of stages) and, for each sampled solution, a Matlab routine (the black-box) works out the cycle design and performance indexes. Compared to the equation oriented approach, such black-box strategy may considerably increase the probability of determining the global optimum because the optimization level considers only the independent decision variables (a few ones) and design specification constraints, since all the dependent variables and unit equations are hidden into the design model (black-box). Due to the objective function discontinuities caused by the turbine design model when automatically changing the number of stages (see Section 5), a derivative-free method suitable for non-smooth black-box problems must be adopted. Among the available methods, PGS-COM, the hybrid derivative-free algorithm recently proposed by Martelli & Amaldi [6], was selected because of its superior performance on discontinuous black-box problems.

The design model and Matlab solution routine are described in Section 4, while the derivative-free optimization algorithm (PGS-COM) is outlined in Section 5.

4. Design and economic model

In this section, we detail the model that given the independent design variables (p_{EVA}, p_{COND}, ΔT_{SH}, $\Delta T_{PP,REG}$, $\Delta T_{PP,MHE}$, ω, β_i) carries out the steady-state simulation (solving the energy and mass balance equations), the preliminary design (sizing the equipment units) and the economic evaluation (computing the capital and operating costs, and the revenue) of the plant.

4.1. Design model

The input of the model is made of the following set of parameters:

- the problem specifications listed in Section 3 (the elemental composition, moisture content, and lower heating value of fuel, the nominal demand of thermal power by the heat user, the expected number of equivalent hours per year, the inlet and outlet water temperatures required by the heat user, the

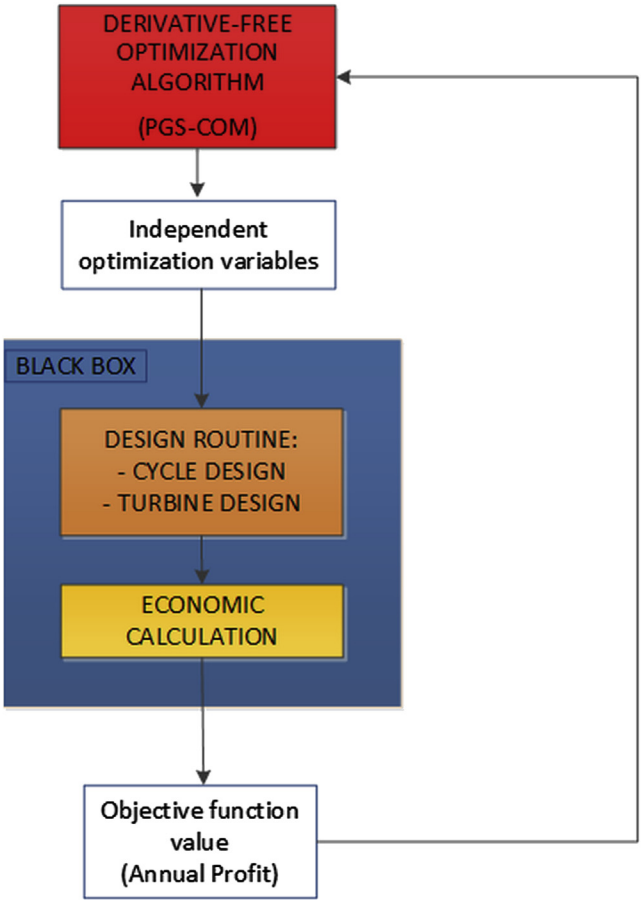

Fig. 6. Block-flow scheme of the proposed black-box optimization methodology.

economic data related to the operation of the plant, the financial assumptions of the investment),
- the independent design variables,
- the assumptions on the performance of the equipment units listed in Table 1.

It is important to note that the design model proposed in this first part of the work (Part A) is based on two strong assumptions: (i) all the condenser thermal power is supplied to the heat user (i.e., there is not an auxiliary condenser/cooler which rejects heat to the environment), (ii) the plant load is controlled so as to exactly match the demand of the heat user. As a consequences of (i) and (ii), the plant cannot be oversized with respect to the power required by the heat user, and the number of full-load equivalent hours of the ORC plant is essentially equal to the number of full-load equivalent hours of the heat user (because the plant is turned-off when there is not demand of heat, and its load is controlled so as to follow the heat demand profile).

The block-flow diagram of the design routine is represented in Fig. 7. A first guess of the turbine isentropic efficiency must be made at the beginning in order to determine the thermodynamic conditions (pressure, temperature and enthalpy) of the cycle streams. Indeed, for given $\Delta T_{PP,REG}$, the regenerated liquid temperature depends on the turbine outlet temperature. Then, the mass flow rates of fuel, air, flue gases, hot oil, working fluid and water are computed on the basis of the specified thermal power demand of the heat user. At this point, since the turbine inlet conditions and flow rate are known, the turbine stages are designed and the actual turbine isentropic efficiency is computed. The sequence of calculation steps

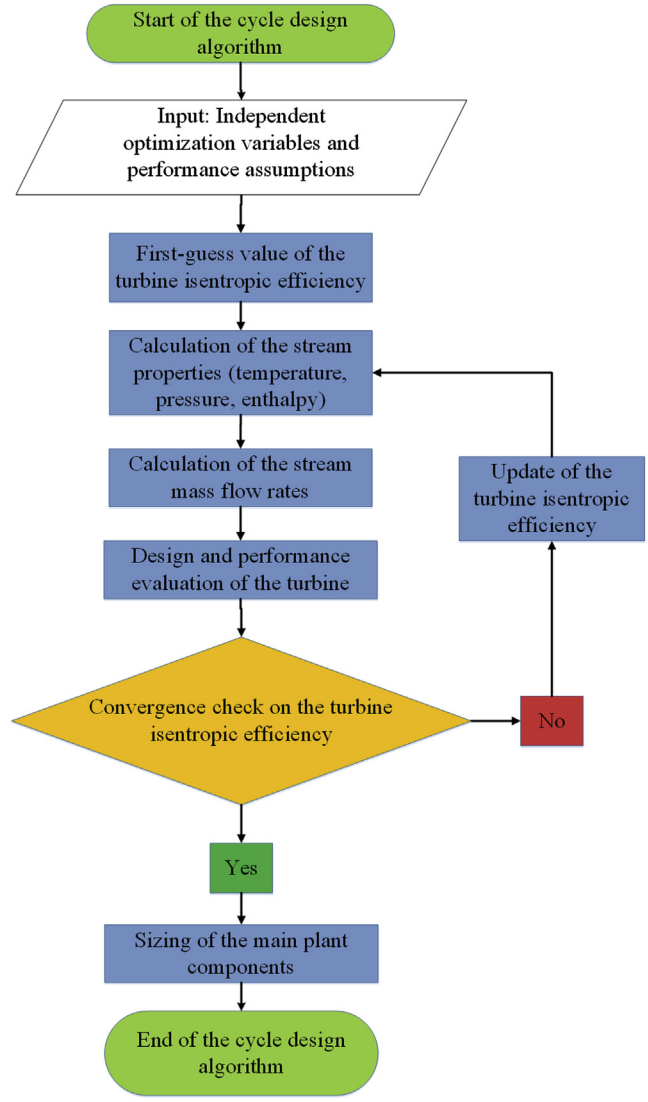

Fig. 7. Block flow diagram of the cycle and turbine design procedure.

(calculation of thermodynamic conditions, flow rates, and turbine design) is repeated until the turbine isentropic efficiency stabilizes to a value (within a specified tolerance).

The calculation of the thermodynamic conditions (temperatures, pressures and enthalpies of flue gases, hot oil, working fluid, and water) corresponding to the input parameters (independent design variables and performance assumptions in Table 1) is not

Table 1
Input performance parameters of the thermodynamic model of the cycle, and their values used in the test cases described in Section 6.

Input performance parameter	Value
Thermal oil temperature at the outlet of the boiler (T_{V2}), °C	300
Percent excess air of the boiler, %	80
Hydraulic efficiency of ORC pump, %	80
Mechanical efficiency of ORC pump, %	0.89
Electric efficiency of ORC pump electric motor, %	0.89
Electric efficiency of ORC elec. generator, %	0.96
Mechanical efficiency of ORC turbine, %	0.96
Boiler heat loss, % of fuel thermal power	3
Regenerator heat loss, % of hot side thermal power	2
Pressure drops of HXs, kPa	50
Minimum boiler stack temperature, °C	120

detailed here for the sake of brevity. However, it is worth noting that we used REFPROP [45], a commercial software using properly calibrated equations for the thermodynamic and transport properties of a wide variety of pure fluids and mixtures, to have accurate estimates of the working fluid properties. The equations of state proposed in Refs. [46], [47] are used for MDM and toluene respectively.

In the following we describe the procedures for calculating the mass flow rates of fluids, the turbine design, the size and cost assessment of the equipment units.

4.1.1. Calculation of the mass flow rates of streams

The working fluid flow rate $\dot{m}_C$ is obtained from the energy balance equation of the condenser:

$$\dot{m}_C = \frac{\dot{Q}_{COND}}{(h_{C10} - h_{C1})}, \tag{10}$$

where h_{C10} and h_{C1} are the enthalpies of working fluid at respectively inlet and outlet of the condenser, and $\dot{Q}_{COND}$ is the condenser thermal power (equal to the specified $\dot{Q}_{USER}$). Then, the hot oil flow rate can be determined by imposing the energy balance equations relative to the two key sections of the main heat exchanger. Indeed, the mass flow rate of hot oil required to generate $\dot{m}_C$ depends on the position of the pinch point within the heat exchanger. According to the analysis of Martelli et al. [38], there are two possible cases: (a) the minimum temperature difference (pinch point) between thermal oil and the working fluid occurs at the admission of the evaporator (see Fig. 8(a)), (b) the pinch point occurs at the cold side of the heat exchanger (see Fig. 8(b)).

In case (a) the required hot oil flow rate is set by the energy balance equation of the control volume including evaporator and super-heater,

$$\dot{m}_V^a = \frac{\dot{m}_C \cdot (h_{C7} - h_{C4})}{c_{OIL} \cdot (T_{V2} - T_{V4}) \cdot (1 - \xi_{MHE})} \tag{11}$$

where

$$T_{V4} = T_{EVA} + \Delta T_{PP,\ MHE}, \tag{12}$$

while h_{C7} and h_{C4} denote the working fluid enthalpies at superheater outlet and evaporator inlet, c_{OIL} the hot oil specific heat capacity, T_{V2} the hot oil inlet temperature and ξ_{MHE} the heat loss coefficient of main heat exchanger (specified in Table 1). In Eq. (12), T_{EVA} denotes the evaporation temperature and $\Delta T_{PP,\ MHE}$ the pinch point temperature difference of the main heat exchanger (independent optimization variable).

Once $\dot{m}_V$ has been determined, the thermal oil temperature at the outlet of the heat exchanger T_{V1} can be computed from the energy balance equation of the economizer,

$$T_{V1} = T_{V4} - \frac{\dot{m}_C \cdot (h_{C4} - h_{C3})}{\dot{m}_V^a \cdot c_{OIL} \cdot (1 - \xi_{MHE})}, \tag{13}$$

where h_{C3} denotes the enthalpy of working fluid at the inlet of the main heat exchanger.

In case (b), the mass flow rate of hot oil is determined by the energy balance equation of the overall main heat exchanger:

$$\dot{m}_V^b = \frac{\dot{m}_C \cdot (h_{C7} - h_{C3})}{c_{oil} \cdot (T_{V2} - T_{V1}) \cdot (1 - \xi_{MHE})}, \tag{14}$$

with

$$T_{V1} = T_{C3} + \Delta T_{PP,MHE}. \tag{15}$$

Temperatures T_{V6} and T_{V4} are then obtained from the energy balance equations of the economizer and evaporator.
In order to automatically determine which one of the two cases actually occurs and determine $\dot{m}_V$, the model computes the required mass flow rates of oil according to either case ($\dot{m}_V^a$ and $\dot{m}_V^b$), and takes the maximum value (i.e., among the two requirements set by Eqs. (11) and (14), the tightest of the two must be satisfied):

$$\dot{m}_V = \max\left(\dot{m}_V^a, \dot{m}_V^b\right). \tag{16}$$

Indeed, the case requiring the largest oil flow rate is the one corresponding to the actual pinch point location. It is worth noting that, when the situation changes from once case to the other (i.e., the pinch point changes location), non-differentiability is generated in the efficiency and cost of the plant, making non-smooth the objective function of the optimization problem.

The mass flow rate of water transferring heat from the condenser to the heat user is obtained from the energy balance equation of the condenser:

$$\dot{m}_W = \frac{\dot{Q}_{COND}}{(h_{w3} - h_{w1})}. \tag{17}$$

Once the mass flow rates of working fluid and water are determined, it is possible to compute the pinch point temperature difference of the condenser and check whether it is greater than zero (i.e., the solution is feasible) or a minimum desired value. Indeed, as the optimization algorithm spans the range of condensation pressures and sets p_{COND} to a low value, it may happen that the water and the condensing fluid temperature profiles cross each other, leading to an infeasible design. According to the constraint handling technique of the black-box optimization algorithm PGS-COM (see Section 5), if the condenser pinch point temperature difference is lower than zero or lower than a desired value, the design routine is prematurely stopped and the objective function value (the annual profit) is set to minus infinite (very unattractive solution).

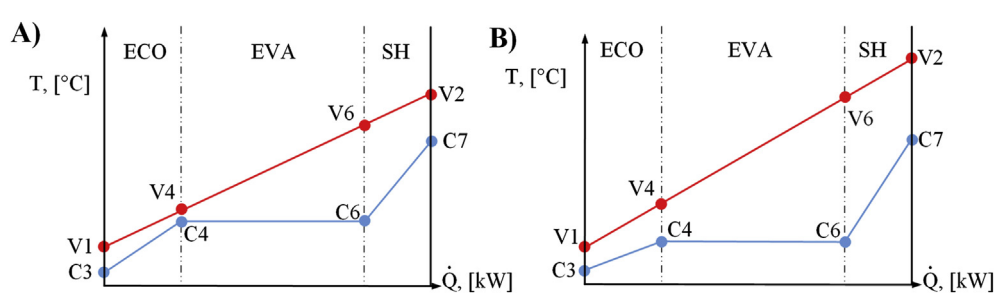

Fig. 8. Possible T-Q (stream temperature vs. exchanged thermal power) diagrams for the main heat exchanger. (A) The pinch point occurs between the economizer and the evaporator. (B) The pinch point occurs at the cold side of the heat exchanger.

Finally, the mass flow rate of flue gases $\dot{m}_F$ and biomass $\dot{m}_{FUEL}$ burned by the boiler can be easily computed from the energy balance equation of the heat exchanger between flue gases and hot oil, and the air-fuel ratio α (which depends on the percentage air excess and fuel composition) respectively:

$$\dot{m}_F = \frac{\dot{m}_v \cdot (h_{V2} - h_{V1})}{(h_{F1} - h_{F2}) \cdot (1 - \xi_B)}, \tag{18}$$

$$\dot{m}_{FUEL} = \frac{\dot{m}_F}{\alpha + 1}, \tag{19}$$

where ξ_B denotes the heat loss coefficient of the boiler, while h_{F1}, h_{F2}, h_{V1} and h_{V2} the enthalpies of flue gases and hot oil at inlet and outlet of the boiler heat exchanger.

4.1.2. Turbine design procedure

The input parameters of the turbine design routine are the admission conditions, the turbine outlet pressure p_{C9} (equal to p_{COND} plus the pressure drops of the regenerator), the working fluid flow rate, the turbine rotational speed and the pressure ratio of each i-th stage β_i, while the output parameters are the number of stages, the enthalpy drop and the isentropic efficiency of each stage and of the overall turbine. Since the number of stages is not known a priori, the pressure ratio β_i is defined for a sufficiently large number of stages $N_{ST,MAX}$ (e.g., >5) with the idea that only a few of them will be necessary. The turbine design algorithm is represented in Fig. 9.

At beginning, the procedure computes the maximum enthalpy drop (work) $\Delta h_{ST,\,MAX}$ achievable by axial stages with maximum total-static efficiency. This value corresponds to the work of an ideal impulse stage with axial outlet velocity designed for the maximum pitch-line velocity u_{MAX} allowed by the rotor material [48]:

$$\Delta h_{ST,\,MAX} = 2u_{MAX}^2. \tag{20}$$

In this work we assumed $u_{MAX} = 255$ m/s, corresponding to $\Delta h_{ST,\,MAX} = 130$ kJ/kg.

Another factor limiting the stage load is the volumetric flow ratio V_{RATIO}, defined as the ratio between the outlet and the inlet volume flow rates:

$$V_{RATIO,i} = \frac{\dot{V}_{OUT,i}}{\dot{V}_{IN,i}}. \tag{21}$$

It is not advantageous to have large V_{RATIO} since it would imply an excessively large increase of the flow velocity and/or flow area which considerably penalize the stage efficiency. According to the results of Macchi and Perdichizzi [35], it is not worth crossing the maximum value $V_{RATIO,MAX}$ of 15.

Once $\Delta h_{ST,\,MAX}$ and $V_{RATIO,MAX}$ have been fixed, the stage design procedure begins from the first stage and proceeds stage-by-stage towards the last one. For each stage i, the outlet pressure $p_{OUT,i}$ is computed from its admission pressure $p_{IN,i}$ and the specified β_i. If $p_{OUT,i}$ is lower than the specified turbine outlet pressure p_{C9}, β_i is decreased imposing that $p_{OUT,i} = p_{C9}$. Knowing the admission conditions and β_i allows to determine the isentropic enthalpy drop $\Delta h_{ISO,i}$. It is worth noting that, due to this approach, the last stage typically has a pressure ratio lower than that specified at input as β_{LAST} is decreased imposing that $p_{OUT,\,LAST} = p_{C9}$.

In order to determine the outlet volume flow rate (i.e., outlet density) and the stage V_{RATIO}, a first-guess value of the stage isentropic efficiency is needed. The first-guess value is then updated after evaluating the actual isentropic stage efficiency with a linear spline interpolation of the results published by Macchi and Perdichizzi [35], $\eta_{ISO,i} = f_{SPLINE}\,(V_{RATIO,i}, N_{S,i}, SP_i)$, which returns the isentropic efficiency of the stage as a function of the volumetric flow ratio, specific speed $N_{S,i}$ and size parameter SP_i of the stage:

$$N_{S,i} = \frac{\omega}{60} \cdot \frac{\sqrt{\dot{V}_{IN,i}}}{\Delta h_{ISO,i}^{3/4}}, \tag{22}$$

$$SP_i = \frac{\sqrt{\dot{V}_{IN,\,i}}}{\Delta h_{ISO,\,i}^{1/4}}. \tag{23}$$

A plot of the linear spline describing the stage isentropic efficiency as a function of specific speed and volume ratio is reported in Fig. 10. The value of $\eta_{ISO,i}$ obtained with the correlation f_{SPLINE} is compared with that assumed at the beginning, and, if the difference is greater than a given threshold value, V_{RATIO} needs to be recomputed. Thus, an iterative algorithm is necessary to update V_{RATIO} and $\eta_{ISO,i}$, until $\eta_{ISO,i}$ stabilizes to a value (within a given tolerance).

The turbine design procedure is prematurely stopped in three cases: (1) if $N_{S,i} > 0.43$ (as the stage efficiency would be too low and the solution would be certainly suboptimal), (2) if $h_{IN,i} - h_{OUT,i} > \Delta h_{ST,\,MAX}$ (as the load is too high for an axial stage), (3) if $V_{RATIO} > V_{RATIO,MAX}$ (excessive increase of flow area and/or flow velocity across the stage). In these cases, also the plant design procedure is stopped and the objective function value (i.e., the annual profit) is set to minus infinite (according to the "extreme barrier approach" used by the optimization algorithm to handle infeasible solutions, see Section 5 and [6]).

4.1.3. Validation of the model equations

The cycle and boiler model described in the previous sections (4.1.1 and 4.1.2) have been validated with the data of real plant, the biomass-fired CHP plant in "Scharnhauser Park", made available by Erhart et al. [49], [50]. The plant scheme is very similar to that reported in Fig. 1. It features a superheated regenerative ORC with MDM as working fluid, 5.3 MW thermal output and 1 MW nominal power output. Design parameters of the "Scharnhauser Park" plant needed for the comparison were taken from Refs. [49], [50] and communicated by the corresponding author (personal communication). Our model predicts about the same cycle gross electric efficiency (14.4%) as well as the same boiler efficiency (81.6%) and working fluid liquid flow rate (30 l/s).

4.1.4. Preliminary design of the equipment units

Once all the mass flow rates and the thermodynamic properties of the streams have been determined, the plant performance and the size of the equipment units can be computed:

$$\dot{W}_{EL,T} = \dot{m}_C \cdot (h_{C8} - h_{C9}) \eta_{MEC,\,T}\, \eta_{EL,T}, \tag{24}$$

$$\dot{W}_{EL,P} = \frac{\dot{m}_C \cdot (h_{C2} - h_{C1})}{\eta_{IDR,\,P} \cdot \eta_{EL,\,P} \cdot \eta_{MEC,\,P}}, \tag{25}$$

$$\dot{W}_{EL} = \dot{W}_{EL,T} - \dot{W}_{EL,P} - \dot{W}_{EL,AUX}, \tag{26}$$

$$\eta_{EL} = \frac{\dot{W}_{EL}}{\dot{m}_{FUEL} \cdot LHV_{FUEL}}, \tag{27}$$

where $\dot{W}_{EL,T}$ and $\dot{W}_{EL,P}$ denote the electric power output of turbine and pump, $\eta_{IDR,\,P}$, $\eta_{MEC,P}$ and $\eta_{EL,P}$ denote respectively the hydraulic, mechanical and electric efficiency of the pump, while $\eta_{MEC,\,T}$ and $\eta_{EL,T}$ the mechanical and electric efficiency of the

1) Set to zero the actual number of stages: $N_{ST} = 0$, set the maximum volumetric flow ratio $V_{RATIO,MAX}$, and compute the maximum allowed stage load $\Delta h_{ST,MAX}$ for the given maximum allowed pitch-line rotor velocity u_{MAX}: $\Delta h_{ST,MAX} = 2u_{MAX}^2$

2) For each stage i =1, 2, … $N_{ST,MAX}$

2.1) compute the outlet pressure of the stage: $p_{OUT,i} = \max\left(\frac{p_{IN,i}}{\beta_i}, p_{C9}\right)$

2.2) determine the corresponding isentropic enthalpy drop: $\Delta h_{ISO,i} = h_{IN,i} - h(p_{OUT,i}, s_{IN,i})$

2.3) evaluate the specific speed of the stage: $N_{S,i} = \frac{\omega}{60} \cdot \frac{\sqrt{\dot{V}_{IN,i}}}{\Delta h_{ISO,i}^{3/4}}$

2.4) compute the isentropic efficiency of the stage

if $N_{S,i} \leq 0.43$,

2.4.1) assume a first-guess value of stage isentropic efficiency $\eta_{ISO,i}$ (e.g., 90%)

2.4.2) compute stage outlet enthalpy $h_{OUT,i}$ and volumetric flow $\dot{V}_{OUT,i}$

$$h_{OUT,i} = h_{IN,i} - \Delta h_{ISO,i} / \eta_{ISO,i}$$

2.4.3) compute stage volumetric ratio $V_{RATIO,i} = \frac{\dot{V}_{OUT,i}}{\dot{V}_{IN,i}}$ and size parameter $SP_i = \frac{\sqrt{\dot{V}_{IN,i}}}{\Delta h_{ISO,i}^{1/4}}$

2.4.4) determine stage isentropic efficiency with linear spline interpolation of the results in [35]: $\eta_{ISO,i} = f_{SPLINE}(V_{RATIO,i}, N_{S,i}, SP_i)$

2.4.5) update $\eta_{ISO,i}$ and go back to step (2.4.2) until $\eta_{ISO,i}$ stabilizes to a value within a given tolerance

else ($N_{S,i} > 0.43$, the stage efficiency would be excessively low and the solution would certainly be suboptimal)

2.4.6) the design procedure is stopped and the objective function value (net plant efficiency or annual profit) is set to minus infinite

2.5) Check on the maximum stage load $\Delta h_{ST,MAX}$ and maximum stage volumetric ratio $V_{RATIO,MAX}$:

2.5.1) if $h_{IN,i} - h_{OUT,i} > \Delta h_{ST,MAX}$ (stage load too high) or if $V_{RATIO} > V_{RATIO,MAX}$ (excessive increase of flow area and/or flow velocity across the stage), the design procedure is stopped and the objective function value (net plant efficiency or annual profit) is set to minus infinite

2.6) Update the actual number of stages: $N_{ST} = N_{ST} + 1$

if $p_{OUT,i} > p_{C9}$ (another stage is necessary to reach the specified turbine outlet pressure)

2.6.1) set $p_{IN,i+1} = p_{OUT,i}$ and $h_{IN,i+1} = h_{OUT,i}$ and go to step (2.1) to define the next stage

else (the turbine design is completed)

2.6.2) Exit the turbine design algorithm and return the output parameters

Fig. 9. Pseudocode of the turbine design algorithm.

turbine. $\dot{W}_{EL,AUX}$ denotes the electric power absorbed by auxiliary units (water pump, oil pump, etc).

Finally a preliminary sizing of all the heat exchangers is done on the basis of their thermal duty, the heat transfer coefficients reported in Table 2, and assuming a counter-current flow arrangement.

4.2. Economic model

In this section we detail the economic model used to evaluate the annual profit of the plant. The investment costs of the main equipment units (including installation), except for the turbine, are computed according to the well-known scaling law,

$$C_i = C_{0,i} \cdot \left.\frac{RS_i}{RS_{0,i}}\right)^{sf}, \tag{28}$$

where C_i denotes the actual investment cost of the i-th unit with size RS_i, $C_{0,i}$ the cost of the unit with reference size $RS_{0,i}$, and sf is the scale factor. The values of these parameters for each equipment unit and the associated reference are detailed in Table 3.

For the turbine, we have used the following correlation which takes into account of the number of stages, the size parameter of the last stage and the mechanical power output:

$$C_T = C_{0,T} \cdot \left(\frac{N_{ST}}{N_{ST,0}}\right)^{0.5} \cdot \left(\frac{SP_{LAST}}{SP_{LAST,0}}\right)^{0.1} \cdot \left.\frac{\dot{W}_{MEC}}{\dot{W}_{MEC,0}}\right)^{0.45}, \tag{29}$$

with $C_{0,T} = 1000$ k€, $N_{ST,0} = 2$, $SP_{LAST,0} = 0.02$ m, $\dot{W}_{MEC,0} = 700$ kW.

Compared to the cost correlation proposed by Astolfi et al. [34], this one considers the turbine power output and is derived for smaller size turbine (in the range 500 kW–2 MW). On the other hand, it is important to note that the cost coefficients have been determined on the basis of a few confidential data, and a more thorough statistical analysis is required. Indeed, this work is mainly focused on the optimization methodology and algorithms, and the cost models have not been reviewed in detail.

In addition to the purchase and installation costs of the cycle components, other costs, such as civil works, contingencies, engineering and procurement, must be included. All these costs, grouped in the cost C_B, typically are considered to be proportional to the total component cost. Instead the cost of permits C_P is assumed to be constant (not proportional to the total cycle cost). The fixed operation and maintenance costs C_M are assumed to be equal to a percentage of the total cycle cost, while the variable operation costs are assumed to be negligible compared to the fuel

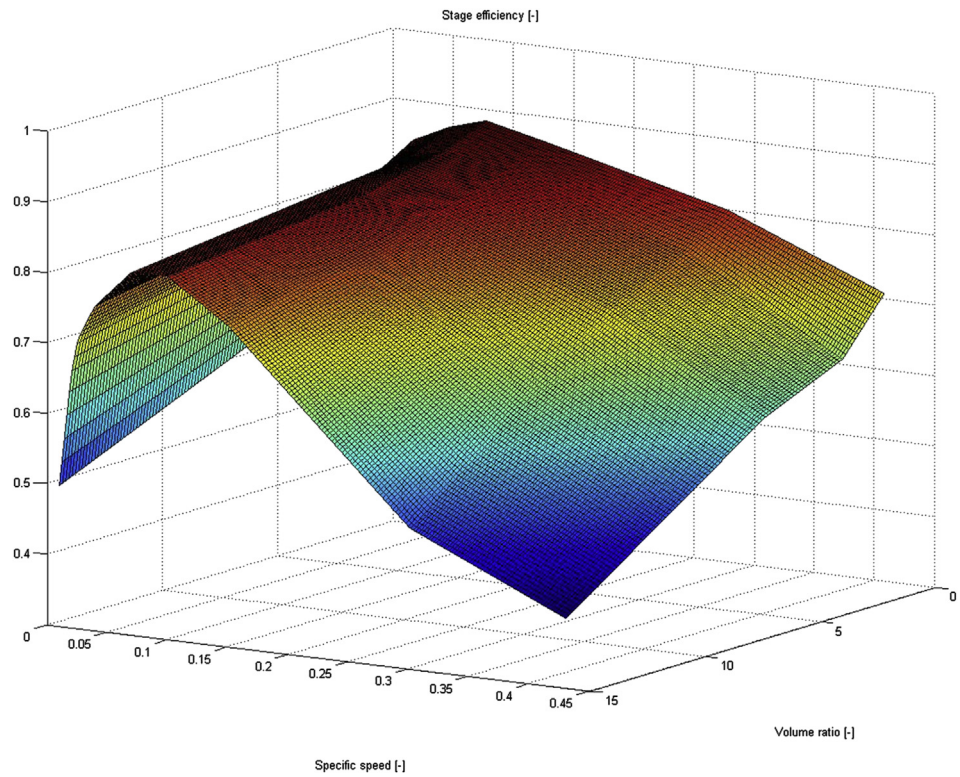

Fig. 10. 3-D plot of the turbine stage isentropic efficiency as a function of N_S e V_{RATIO}. The function is obtained by interpolating the results of [35] with a linear spline.

Table 2
Set of global heat transfer coefficients needed by the design model and values used in the test cases described in Section 6.

Heat exchanger	Global heat transfer coefficient [kW/(m^{2}K)]	Reference
Condenser	550	[50]
Regenerator	120	[51]
Superheater	120	[51]
Evaporator	350	[51]
Economizer	350	[51]
De-superheater	150	[51]

cost C_{FUEL}. The annual profit P is computed by converting the total plant cost into an annual cost with the Levelized Capital Charge Rate LCCR [43], and subtracting costs to revenues:

$$P = sp_{EL}\,E_{EL} + sp_Q\,Q_{USER} - \left(C_B + C_P + \sum_{j\in\Phi} C_j\right)\cdot LCCR - C_M - C_{FUEL}, \tag{30}$$

where sp_{EL} is the electricity selling price, sp_Q is the heat selling price, Q_{USER} is the total heat supplied to the user, Φ labels the set of equipment units of the plant, and C_j the investment cost of the j-th equipment unit. The LCCR is defined as the amount of revenue per unit of investment cost that is needed to pay the carrying charges on that investment (return on investment, income and property tax, book depreciation, and insurance). The detailed calculation procedure is reported in Ref. [43]. LCCR multiplied by the total capital investment gives the annual cost of the investment.

Q_{USER} depends on the number of full-load equivalent hours of the heat user Nh_{EQ},

$$Q_{USER} = \dot{Q}_{USER} Nh_{EQ}, \tag{31}$$

and E_{EL} is the total electric energy generated over one year,

$$E_{EL} = \dot{W}_{EL}\,Nh_{EQ}. \tag{32}$$

Similarly C_{FUEL} is computed on the basis of the fuel specific cost pc_{FUEL} and the fuel mass flow rate:

$$C_{FUEL} = pc_{FUEL}\dot{m}_{FUEL} LHV_{FUEL} Nh_{EQ}. \tag{33}$$

Table 3
Parameter values of the cost estimation models used for each piece of equipment.

	Scaling parameter	C_0 [k€]	RS_0	sf	Source
Main Heat Exchanger	U*S [W/K]	1500	4000	0.9	Astolfi et al. [34]
Regenerator	U*S [W/K]	250	650	0.9	Astolfi et al. [34]
Boiler	Fuel thermal power [MW]	2000	6.5	0.875	Private communication by the engineering company “ITI Engineering”.
Condenser	Area [m^2]	530	3563	0.9	Estimated with Thermoflex [52]
Electric generator	Electric power [kW]	200	5000	0.67	Astolfi et al. [34]
Pump	Electric power [kW]	14	200	0.67	Astolfi et al. [34]

5. Design optimization problem and algorithm

The plant model described in Section 4 is used as a black-box function within the following optimization problem (P1):

$$\begin{aligned} &\max_{\boldsymbol{x}_D} \; P(\boldsymbol{x}_D) \\ &\text{s.t.} \;\; \boldsymbol{g}_D(\boldsymbol{x}_D) \le 0 \\ &\boldsymbol{lb}_D \le \boldsymbol{x}_D \le \boldsymbol{ub}_D \\ &\boldsymbol{x}_D \in \mathscr{R}^{n_D} \end{aligned} \tag{P1}$$

where the objective is to maximize the annual profit P defined in Eq. (30) and computed by the design model, and the decision variables $\boldsymbol{x}_D$ are p_{EVA}, p_{COND}, ΔT_{SH}, $\Delta T_{PP,REG}$, $\Delta T_{PP,MHE}$, Q_{COND}, ω, and β_i of each turbine stage. Problem (P1) features lower and upper bounds ($\boldsymbol{lb}_D$ and $\boldsymbol{ub}_D$) on the deaign variables (physical and technological limitations) and a set of nonlinear black-box (computed by the design model) design constraints $\boldsymbol{g}_D$ corresponding to:

- the heat transfer feasibility within the condenser (i.e., the condition that the pinch point temperature difference of the condenser must be greater than zero),
- the maximum load, specific speed or volumetric expansion ratio of the turbine stages (Fig. 9).

Only these constraints must be included in the optimization problem since all the physical equations (i.e., mass and energy balance equations) are guaranteed by the plant model (within the black-box). It is worth noting that the objective function value is not defined in some points of the solution space defined by the bounds. Indeed, in the points where one of the constraints $\boldsymbol{g}$ is not satisfied, the black-box fails to return the objective function value since the cycle design model or turbine design prematurely stop. Moreover, the objective function is also (1) discontinuous, due to the turbine design procedure which automatically changes the number of stages causing discontinuities in the cycle performance and cost, and (2) non-differentiable, due to the "max" operator used to compute the oil mass flow rate in Eq. (16) and the linear spline interpolation used to assess the turbine stage efficiency. For instance, Figs. 11 and 12 show 3-D plots of the net electric efficiency and annual profit of the ORC plant considered as test case in Section

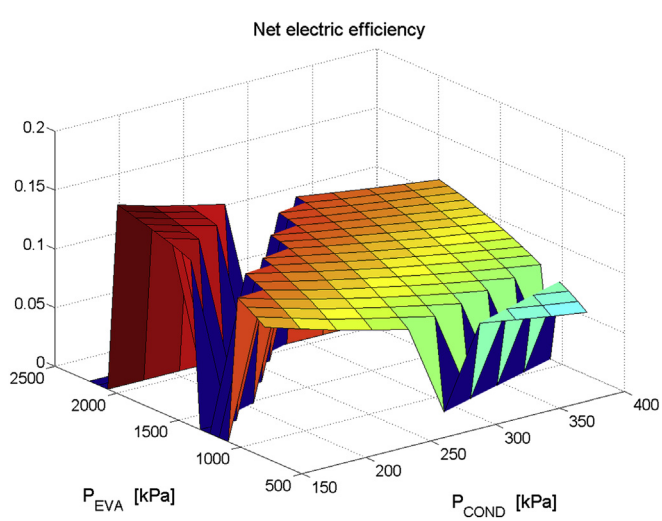

Fig. 11. 3-D plot of the net electric efficiency of the ORC plant considered in Section 6 as a function of the evaporation and condensation pressures. It important to note that the function is not defined over the whole variable space because for some combi-nations of evaporation and condensation pressures the turbine design turns out to be infeasible.

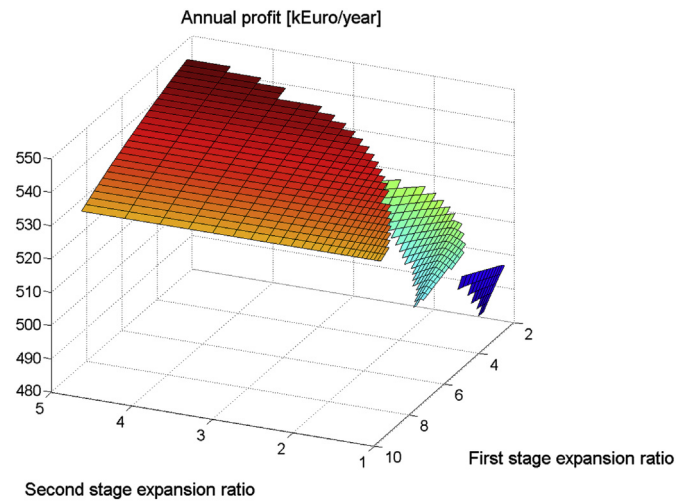

Fig. 12. 3-D plot of the annual profit of the ORC plant considered in Section 6 as a function of the first and second stage pressure ratio. It important to note that the function has step-type discontinuities corresponding to the activation of turbine stages (which imply an increase of investment cost).

6. They show the extremely non-smooth nature of the black-box function and the presence of regions where the objective func-tion is not defined. For these reasons, an effective and robust direct-search algorithm must be used.

Among the available direct-search methods, we selected PGS-COM, the hybrid method specifically developed by Martelli and Amaldi [6] for non-smooth black-box problems. This algorithm combines the positive features of the CPSO (Constrained Particle Swarm Optimizer) of Hu and Eberhart [53], GSS (Generating Set Search) of Lewis et al. [54], and the Complex of Andersson [55]. Each iteration of the algorithm consists of three steps: (i) a search step corresponding to a population update of a revised CPSO, (ii) an optional (skipped if the CPSO improves the best solution found so far) poll step corresponding to an iteration of the GSS around the best solution found so far, and (iii) a few optional (skipped if either the CPSO or the GSS step finds a better solution) reflection steps corresponding to a few iterations of the Complex algorithm. The algorithm stops when the swarm size (defined as the maximum distance between the best particle and the remaining particles), the step size parameter of the GSS step and the size of the population used by the Complex step become smaller than given threshold or the maximum number of function evaluations is reached. The main idea is to exploit the effectiveness of the population-based CPSO algorithm to rapidly identify promising regions of the set of the feasible solutions, and then take advantage of the effectiveness of the Complex search for non-smooth problems (see Ref. [6] for further details) to intensify the search in selected sub-regions. The GSS step is used to generate the starting solutions for the Complex step, and to improve the algorithm robustness towards numerical noise in the objective function (as GSS is more robust than Complex). The algorithm is also coded for parallel computing as the function evaluations performed by the CPSO and GSS steps are parallelized taking advantage of multiple core computers. The computational results presented in Ref. [6] indicate that for noisy non-smooth black-box problems PGS-COM performs better than eleven ad-hoc methods. As far as the parameter values of the algorithm are concerned (e.g., number of swarm particles, neighborhood size, minimum GSS step size parameter, etc), in this work we have adopted the same values recommended by the authors in Ref. [6]. The unrelaxable hidden nonlinear constraints $\boldsymbol{g}_D$ have been handled with the extreme barrier approach (i.e., if one of them is

Table 4
Design specifications, boundary conditions and economic data of the test case.

Parameter	Value
Electricity revenue (€/MWh)	80/110/140
Heat revenue (€/MWh)	60
Fuel cost (€/MWh)	18
Temperature of hot oil (°C)	300
Temperature of hot water to the user (°C)	80
Number of full-load equivalent hours of the heat user (h)	4290
Nominal thermal power (kW)	5300
Temperature of air (°C)	25

violated, the objective function value is set to minus infinite so as to penalize that solution), as recommended in Ref. [6]. Since the black-box evaluation is not particularly time expensive (it takes about 0.25 s on a workstation equipped with 3.4 GHz Intel i7-3770 pro-cessor) and the possibility of exploiting parallel computing on 4 cores, the maximum number of function valuations was set to 20,000. Moreover, because of the stochastic nature of the algorithm and the possible influence of the starting solutions on the returned solution, each optimization has been repeated 10 times from randomly generated starting points. As for the stopping criterion, the maximum number of function evaluations and a convergence tolerance of 10^{-6} on the three search steps were considered.

6. Test case

In this section the proposed design optimization algorithm is tested on a real-world problem: optimize the design of a biomass-fired CHP ORC for a district heating network of a residential area. The plant must supply 5.3 MW of thermal power to the district heating for a number of full-load equivalent operating hours equal to 4290 (the same as the ORC plant described in Ref. [56]). The design specifications and boundary conditions are reported in Table 4. The input parameters of the design model are reported in Tables 1 and 2, while those of the economic model are reported in Table 4. The optimization is repeated for three different electricity prices (80, 110 and 140 €/MWh) in order to show the effect of such parameter on the optimal cycle design.

As far as the selection of the working fluid is concerned, for the sake of brevity, we report and compare the optimization results relative to two fluids adopted in commercially available ORC units, toluene and MDM [23].

The upper and lower bounds of the independent optimization variables (those optimized by PGS-COM) are indicated in Table 5. The most critical bounds are discussed in this paragraph. The evaporation pressure must be within 300 kPa (which is a very low limit) and the critical pressure of the fluid (to have a subcritical cycle). The superheating degree must be within 1 K (just to guarantee the complete evaporation of the fluid) – 75 K (high value which should never be reached). The pinch point temperature difference of the main heat exchanger and regenerator are inferiorly bounded at 1 K and superiorly at 70 K (very high value). Please note that in the case of the regenerator, it is important to set the upper bound of its pinch point temperature difference to a sufficiently large value in order to allow the optimizer to deactivate it. Other critical bounds are the lower bound on the condenser pressure, and the upper bound on the turbine rotational speed. The former is set to 10 kPa on the basis of the features of the commercially available vacuum and sealing systems. Instead, the latter is set at 20,000 rpm, so as to limit the cost of the gear-box needed to match the turbine with the electric generator.

In addition to the bounds on the independent optimization variables, a constraint on the pinch point temperature difference of the condenser is defined so as to keep it positive and above 1 K.

6.1. Max efficiency design

Before determining the design with maximum annual profit, it is worth determining the one with maximum net electric efficiency in order to validate the overall approach (design models and optimization algorithm). Indeed, thanks to well-known thermodynamic criteria, it is quite straightforward to figure out the optimal values of some design variables, such as, the pinch point temperature differences of the heat exchangers, and the number of turbine stages. Since turbine cost is not penalized, the number of turbine stages is limited to a maximum of three by adding a constraint to the optimization problem. Indeed, without such a constraint, the optimizer would move towards solutions with extremely low stage loads (thus with many stages) in order to maximize the turbine expansion efficiency. The constraint is implemented in the black-box as an "unrelaxable constraint" (if violated, the objective function value, i.e., the net plant efficiency, is set to zero), as recommended for the PGS-COM algorithm [6]. As for the minimum pinch point temperature differences of the heat exchangers, a value of 1 K is considered. On the basis of these constraints and the well-known thermodynamic criteria, the maximum efficiency design is expected to have the pinch point temperature differences of the heat exchangers as well as the condenser pressure at their lower bounds, and three turbine stages.

The convergence curve (objective function value as a function of the number of function evaluations) of the algorithm for one run is shown in Fig. 13, while the optimization results are reported in Table 6. The computational time required by the optimization algorithm with parallel computing on 4 cores is about 3 min. It is important to note that in all the 10 runs the algorithm convergence curves resemble that of Fig. 13 and the algorithm returns the same optimal solution (with only minor variations).

The optimization algorithm correctly sets the temperature differences of the heat exchangers at their lower bounds. The condenser pressure is set to the lower value allowed by the bounds (for MDM) or the water loop temperature (for toluene). Indeed in the case employing toluene, the pinch point temperature difference is at the lower bound (1 K). Instead, in the case using MDM, the

Table 5
Upper and lower bounds on the independent optimization variables.

	Lower bound	Upper bound
Evaporation Pressure, kPa	300	Critical pressure
Superheating degree, K	1	75
Pinch point temperature diff. of the MHE, K	1	70
Pinch point temperature diff. of the regenerator, K	1	70
Condenser pressure, kPa	10	200
Turbine rotational speed, rpm	1000	20,000
Stages expansion ratio (–)	1	20
Constraint on the condenser pinch point temperature difference, ≥1 °C		

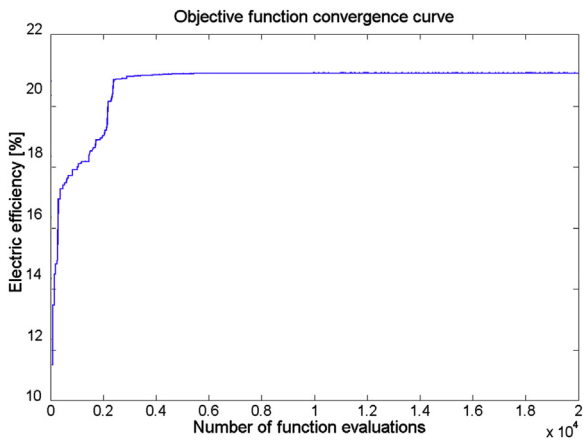

Fig. 13. Convergence curve of PGS-COM relative to the maximum efficiency test case.

condenser pinch point temperature difference is 3.4 °C because the condenser pressure is inferiorly bounded by the pressure limit (10 kPa). For both fluids, the optimized design uses a superheated regenerative cycle. It is worth noting that the evaporation pressure, even if high, is not at the upper bound (critical pressure of the fluid) and the superheating degree is not minor but considerable. Compared to the solution with maximum (or supercritical) evaporation pressure and minimum superheating degree (which would be optimal without regenerator), the returned solution allows to (i) better exploit the regenerator by preheating the liquid to a higher temperature, and then reduce the boiler fuel consumption, (ii) have higher turbine isentropic efficiency because of the limited expansion ratio of the stages.

As far as the turbine design is concerned, the optimization algorithms exploits all the (three) available turbine stages and chooses different values of expansion ratios for each stage. The stage expansion ratio increases through the stages, so as to balance the load coefficients (i.e., stage enthalpy drop divided by $\omega^2 D^2$) of the three stages. Details of the turbine design and performance are reported in Table 7.

As far as the comparison between the two fluids is concerned, it is interesting to note that toluene allows to reach a higher electric efficiency compared to MDM, the opposite result of what was found in the preliminary thermodynamic analysis of the ideal cycles (Section 2). This is mainly due to the technical constraint which does not allow to decrease the condensation pressure below 10 kPa and the higher isentropic efficiency of the turbine stages. Indeed, the condensation temperature of the MDM cycle is higher than that of toluene and this affects the cycle efficiency. Another advantage of toluene over MDM is the lower turbine expansion ratio implying lower stage volumetric ratios, and, in turn, higher isentropic stage efficiencies (see Table 7). In addition, thanks to the greater heat of evaporation, toluene needs a smaller mass flow rate. On the other hand, due to its lower molecular weight, toluene has larger stage loads (actual enthalpy drops). As a consequence of the higher stage loads and lower volumetric flow rates, the optimal rotational speed for toluene is much higher than that of MDM, and it is practically at the upper bound.

Cost-related differences between the designs with toluene and MDM are discussed in the next subsection.

Table 7
Details of the turbine optimized for maximum plant efficiency.

	Stage 1	Stage 2	Stage 3
Maximum efficiency design with MDM			
Expansion ratio	3.446	3.202	10.917
Specific speed	0.046	0.095	0.100
Iso-entropic enthalpy drop, kJ/(kg K)	19.344	20.998	43.934
Actual enthalpy drop, kJ/(kg K)	15.963	18.263	36.520
Volume ratio	4.778	3.373	10.843
Stage efficiency	0.825	0.870	0.831
Size Parameter, m	0.011	0.023	0.036
Maximum efficiency design with toluene			
Expansion ratio	2.269	3.598	7.025
Specific speed	0.065	0.070	0.100
Iso-entropic enthalpy drop, kJ/(kg K)	32.905	55.770	83.689
Actual enthalpy drop, kJ/(kg K)	28.291	47.827	70.913
Volume ratio	2.609	3.731	6.679
Stage efficiency	0.860	0.857	0.847
Size Parameter, m	0.008	0.012	0.020

6.2. Maximum profit design

Design optimization has been repeated considering the annual profit as objective function, and the number of equivalent full-load heating operating hours of the district heating network.

As for the algorithm convergence behavior, the computational time and convergence curves are similar to those registered for the maximum efficiency designs.

The optimization results are presented and compared to those of the maximum electric efficiency design in Table 8. EFF labels the

Table 6
Optimization results (optimization variables and performance indexes) of the maximum-efficiency designs.

	Toluene	MDM
Evaporation Pressure, kPa	2293	1204
Evaporation Temperature (dependent variable), K	546	553
Superheating degree, K	26.4	18.8
Pinch point temp. diff. of MHE, K	1.0	1.0
Pinch point temp. diff. of regenerator, K	1.0	1.0
Condenser pressure, kPa	40.0	10.0
Pinch point temp. diff. of condenser (dependent variable), K	1.0	2.6
Turbine rotational speed, rpm	19998.9	8269.9
Number of turbine stages (dependent variable)	3	3
First stage expansion ratio	2.269	3.446
Second stage expansion ratio	3.598	3.202
Third stage expansion ratio	7.025	10.917
Electric efficiency (objective function), %	21.898	21.327
Net electric power output (dependent variable), kW	1805.1	1782.5
Fuel thermal input LHV basis (dependent variable), KW	82430.0	83578.4
ORC mass flow rate (dependent variable), kg/s	13.86	28.73
Hot Oil mass flow rate (dependent variable), kg/s	53.19	61.58
Thermal efficiency (dependent variable), %	64.30	63.41

design optimized for maximum electric efficiency, PR-80, PR-110 and PR-140 label the designs optimized for maximum profit with electricity selling price p_{EL} equal to 80, 110 and 140 €/MWh, respectively. Table 9 reports the details relative to the turbine stages for cases PR-140.

It is important to note that for both fluids designs PR-80 turn out to have a rather poor efficiency because, due to the low electricity price, they have been arranged for the minimum investment cost. Indeed, the electricity price is so low that using just a boiler would be more advantageous (leading to an annual profit of about 500 k€/y). For both toluene and MDM the optimized turbine employs only one stage and, as a result, the evaporation and condensation pressure are kept close each other so as not to exceed the limit on the stage volumetric flow ratio (which turns out to be the tightest constraint limiting the stage load). In addition, the pinch point temperature differences of the heat exchangers are set to fairly large values so as to save heat exchange area.

As far as toluene is considered as working fluid, there are small differences between the optimized designs PR-110 and PR-140. Indeed, both designs employ the minimum allowed pinch point temperature difference of the main heat exchanger, close-to-minimum pinch point temperature differences of condenser, fairly higher pinch point temperature differences of the regener-ator, about 25–30 °C of superheating degree, and a two-stage turbine. Compared to the maximum efficiency design (EFF), PR-110 and PR-140 use two stages (instead of three), slightly higher condenser pressures (to limit the investment cost of the condenser) and pinch point temperature differences, and a slightly lower evaporator pressure.

In all cases employing toluene the optimal rotational speed of the turbine is at the upper bound because of the high stage enthalpy drops and small volumetric flow rates.

As far as MDM cycles are considered, there are major differences between case PR-110 and PR-140. PR-140 has much more aggressive cycle variables (pressures and temperatures) compared to PR-110. This is mainly due to the different number of turbine stages. Design PR-110, having only one turbine stage (to limit the capital cost), has a low evaporation pressure and a rather high condensation pressure so as not to cross the maximum volume ratio limit of the stage. Except for the turbine design, the cycle design PR-140 (with MDM) closely resembles the maximum efficiency design EFF. With respect to the turbine of design EFF, PR-140 has two stages and a higher rotational speed so as to compensate the higher loads of the stages.

It is worth noting that for both working fluids, design PR-140 has a higher annual profit than design EFF thanks to the cheaper turbine design which leads a lower investment cost. Another common feature of the two fluids is the surprisingly low optimal pinch point temperature difference of the MHE, which for high electricity prices turns out to be at the lower bound (1 K). Possible reasons are the high heat transfer coefficients of both fluids (hot oil and organic working fluid) and the fact that the logarithmic mean temperature difference of the MHE is considerably larger than the pinch point temperature difference.

As far as the comparison between the two working fluids is concerned, on the basis of the cost models and economic assumptions adopted in this work, toluene outperforms MDM not only in terms of net electric efficiency but also in terms of economic

Table 9
Details of the turbine optimized for maximum annual profit with electricity price equal to 140 €/MWh.

	Stage 1	Stage 2
Turbine of design PR-140 with MDM		
Expansion ratio	6.567	15.00
Specific speed	0.048	0.10
Iso-entropic enthalpy drop, kJ/(kg K)	32.27	50.28
Actual enthalpy drop, kJ/(kg K)	26.14	41.00
Volume ratio	8.43	15.00
Stage efficiency	0.8099	0.8150
Size Parameter, m	0.099	0.0259
Turbine of design PR-140 with toluene		
Expansion ratio	5.14	10.38
Specific speed	0.038	0.070
Iso-entropic enthalpy drop, kJ/(kg K)	68.95	101.63
Actual enthalpy drop, kJ/(kg K)	55.76	84.90
Volume ratio	6.04	9.90
Stage efficiency	0.808	0.834
Size Parameter, m	0.0063	0.0142

Table 8
Optimization results and performance indexes of the maximum profit designs, and comparison with those obtained by maximizing the net electric efficiency.

Test case	Toluene				MDM			
	EFF	PR-80	PR-110	PR-140	EFF	PR-80	PR-110	PR-140
Evaporation Pressure, kPa	2293	998.7	2287.0	2190.1	1204	399.00	515.49	985.86
Evaporation Temperature (dependent var.), K	546	489.9	539.7	535.37	553	487.3	501.2	525.4
Super heating degree, K	26.4	75.0	26.6	29.8	18.8	0.1	62.8	31.9
Pinch point temp. diff. of MHE, K	1.0	8.3	1.0	1.0	1.0	70.0	9.1	1.0
Pinch point temp. diff. of regenerator, K	1.0	20.1	7.3	4.67	1.0	39.4	9.8	6.6
Condensation pressure, kPa	40.0	66.79	42.23	41.05	10.0	31.24	37.90	10.00
Pinch point temp. diff. of condenser (dependent var.), K	1.0	18.43	3.16	2.09	2.6	39.87	42.65	3.7
Turbine rotational speed, rpm	19998.9	20,000	20,000	20,000	8269.9	17845	19235	10,950
Number of turbine stages (dependent var.)	3	1	2	2	3	1	1	2
First stage expansion ratio	2.269	18.081	5.331	5.139	3.446	15.24	15.4288	6.567
Second stage expansion ratio	3.598	–	10.158	10.381	3.202	–	–	15.005
Third stage expansion ratio	7.025	–	–	–	10.917	–	–	–
Nominal electric efficiency, %	21.898	15.044	20.776	21.011	21.327	9.352	12.666	19.953
Nominal power output, kW	1805.1	1110.90	1680.46	1706.54	1782.5	633.24	916.53	1626.98
Fuel thermal input LHV basis, kW	82430.0	7384.51	8088.60	8122.10	83578.4	6771.16	7235.92	8153.73
ORC mass flow rate, kg/s	13.86	13.25	13.58	13.69	28.73	22.36	26.62	27.44
Oil mass flow rate, kg/s	53.19	29.05	51.91	48.87	61.58	65.20	39.22	49.25
Thermal efficiency, %	64.30	71.77	65.52	65.25	63.41	78.27	73.25	65.00
Investment cost, M€	5.720	4.593	5.292	5.346	6.141	4.234	4.587	5.536
Specific investment cost, €/kW	3168.80	4134.49	3149.14	3132.65	3445.16	6686.25	5004.75	3402.62
Annual profit, k€	666.65	255.86	473.24	691.59	560.02	211.21	319.80	603.47
Payback time	9	18	12	8	11	21	15	10

The annual profit of cases EFF (max efficiency) has been calculated with an electricity selling price of 140 €/MWh so as to compare them with cases PR-140.

performance. Its main advantage over MDM is the larger evaporation enthalpy, which leads to a more compact and less expensive turbine (because of lower volumetric flow rate), as indicated by the lower specific investment cost (defined as total investment cost/net electric power) reported in Table 8. However, the results of this work are not sufficient to identify the best working fluid for the application since other promising fluids should be considered (e.g., MD2M), and additional costs related to safety issues should be included in the model.

7. Conclusions

The main objective of this paper, first part of a two-part publication, was to describe and show the effectiveness of a design optimization approach for Combined Heat and Power Organic Rankine Cycles capable of simultaneously optimizing the cycle and the turbine design variables. First the thermodynamic analysis of Rankine Cycles with dry-expansion fluids is analyzed to identify the effects on the cycle efficiency of the cycle variables. In particular, it is shown that in cycles with regeneration superheating leads to an increase of the electric efficiency and that, for the same maximum and minimum cycle temperatures, MDM appears to be more advantageous than toluene in terms of ideal cycle efficiency. Then, the optimization algorithm and models are described. Within a black-box strategy, an iterative Matlab algorithm (the black-box) compute the cycle and turbine design, while a direct-search derivative-free algorithm (PGS-COM) optimizes the independent design variables. The objective function can be any thermodynamic or economic performance index. In the latter case, cost models of the main equipment units have been included in the Matlab design algorithm. The number of turbine stages is optimized with a turbine model which avoids the use of integer variables by automatically activating/deactivating stages, but, on the other hand, introduces step-type discontinuities in the optimization problem.

The computational results obtained for a medium size biomass-fired Combined Heat and Power Organic Rankine Cycle show that, thanks to PGS-COM, the overall design-optimization algorithm is robust and computationally efficient. Indeed, the same solutions are obtained at each run and, thanks to the parallel-computing capability of PGS-COM and the use of a multiple-core computer, the computational time is of the order of 3 min. This feature makes the approach an effective design tool not only for research but also for the industrial sector. Moreover, the cycle design model and the optimization algorithm are expected to return optimal or close-to-optimal solutions, as verified for the maximum efficiency test case on the basis of well-known thermodynamic criteria.

As for the cycle designs are concerned, the following important results have been found:

1) Performing just thermodynamic analyses based on ideal cycle models (as those done in Section 2) to determine the optimal cycle variables may be misleading as such analyses do not take into account design constraints and actual performance of equipment units. Indeed, while MDM appears to outdo toluene in terms of cycle efficiency according to the thermodynamic analysis of Section 2, the optimization of cycle and turbine variables with detailed models leads to the opposite result: using toluene as working fluid results in higher electric efficiency (+0.56 percentage points when optimizing the cycle for the maximum efficiency) than MDM (reasons are reported below at the third point of this list).
2) For both fluids, the designs optimized for maximum efficiency use a superheated regenerative cycle with subcritical evaporation pressure and appreciable superheating degree. The evaporation pressure is not pushed to the upper bound (the critical pressure) in order to limit the expansion ratio of the turbine stages which have a negative effect on the stage efficiency. The turbine designs exploit all the (three) available turbine stages with increasing expansion ratios, so as to balance the load coefficients of the three stages.
3) Toluene allows to reach higher electric efficiency compared to MDM because of the technological limitation on the condensation pressure and the higher isentropic efficiency of the turbine stages (about +1.5 percentage points) which benefit from lower expansion ratios.
4) Also when optimizing the economic profit of the cycles, toluene outperforms MDM (from 12.7% up to 32.4% of higher annual profit depending on the electricity selling price). The main cost-related advantage of toluene is the larger evaporation heat which guarantees more compact and less expensive turbine and cycle components (due to the smaller volumetric flow rates of the working fluid). The specific investment costs (defined as total investment cost divided by the net electric power) of the optimized cycles using toluene turn out to be between 8% and 35–40 % lower than those of MDM.
5) When maximizing the annual profit of the ORC, the optimal values of the design variables strongly depend on the electricity selling price. The optimal evaporation and condensation pressures depend on the number of turbine stages, which, in turn, mainly depends on the electricity revenue. If a low electricity price is assumed (80 €/MWh), it is not advantageous to use multiple-stage turbines, and the ratio between the evaporation and condensation pressures is upperly bounded by the turbine stage expansion limit. In the investigated fluids, toluene and MDM, the tightest limit is the maximum volumetric flow ratio of the stage. The cycle reaches a very poor net electric efficiency so as to limit the investment cost. Instead, if high electricity prices are considered (140 €/MWh), for both fluids the optimal turbine design has two stages and the cycle variables resembles those of the maximum efficiency design with minor adjustments.

The above-described results provide useful guidelines for designing efficient and cost-effective biomass-fired organic Rankine cycles for combined heat and power generation.

In the second part of this work (Part B [36]) the cycles are re-optimized taking into account also the optimal part-load control strategy, part-load performance and expected operating conditions.

Acknowledgements

This study was economically supported by the Italian Ministry of the Environment and Protection of Land and Sea (CUP F81C07000120003) ("Ministero dell'Ambiente e della Tutela del Territorio e del Mare") within the framework of the research project "CUBIS – Cogenerazione Urbana da Biomasse e Solare" granted to LEAP (Laboratorio Energia Ambiente Piacenza). The authors acknowledge also Marco Astolfi (Postdoc at Politecnico di Milano) for the invaluable advice and interesting discussions about cost models, as well as Marco Resemini (Engineer at ITI Engineering) for providing extremely useful cost data, and LEAP (Laboratorio Energia Ambiente Piacenza) for partially funding the research activity of Federico Capra.

Nomenclature

Acronyms

CHP	Combined heat and Power
CPSO	Constrained Particle Swarm Optimizer
DIRECT	Dividing Rectangle Algorithm

GA	Genetic Algorithm
GSS	Generating Set Search algorithm
LCCR	Levelized capital charge rate
LHV	lower heating value
MDM	otcamethyltrisiloxane working fluid
MHE	Main (Thermal oil-working fluid) heat exchanger
MINLP	Mixed integer nonlinear program
ORC	Organic Rankine cycle
NLP	Nonlinear program
PGS-COM	Pattern Generating Set Complex optimization algorithm
PR	plant designs optimized for maximum annual profit

Symbols

$\boldsymbol{x}$	vector of optimization variables
$\boldsymbol{lb}$	lower bounds of the optimization variables
$\boldsymbol{ub}$	upper bounds of the optimization variables
$\boldsymbol{g}$	vector of inequality constraints of the optimization problem
$\boldsymbol{h}$	vector of equality constraints of the optimization problem
$\dot{m}$	mass flow rate
$\dot{V}$	volumetric flow rate
T	temperature
p	pressure
h	enthalpy
s	entropy
c	specific heat capacity
EX	exergy
η	efficiency
$\dot{W}$	electric power
E	electric energy
$\dot{Q}$	thermal power
Q	heat
ω	turbine rotational speed
β	turbine stage pressure ratio
V	volumetric flow ratio of turbine stages
Ns	Specific speed of turbine stages
SP	Size Parameter of turbine stages
D	diameter of turbine states
u	turbine stage pitch-line speed
N	integer number
ξ	Thermal losses for heat exchangers
U	global heat transfer coefficient of heat exchangers
S	heat transfer area of heat exchangers
α	mass ratio between fuel and air
C	cost
P	annual profit
sp	selling price
pc	purchase cost
sf	scale factor
Φ	set of equipment units of the plant
Nh	number of full-load equivalent hours

Subscripts

A	Air flows
AUX	auxiliaries
B	Boiler
C	working fluid flows
D	design variables
COND	condenser
DESH	Desuperheater
EL	electric
EQ	full-load equivalent (operating hours)+
EVA	evaporator
F	flue gasses
FUEL	biomass input
ISO	isentropic
PP	pinch point
LAST	last stage of the turbine
MEC	mechanical
MHE	main heat exchanger
REG	regenerator
SH	superheater
ST	stage
T	turbine
USER	heat user
TH	thermal
V	Hot oil
W	Water

References

[1] Conboy T, Wright S, Pasch J, Fleming D, Rochau G, Fuller R. Performance characteristics of an operating supercritical CO_2 Brayton cycle. J Eng Gas Turbines Power 2012;134:111703.

[2] Turboden. List of Turboden ORCs installed throughout the world. 2015 [Online]. Available: http://www.turboden.eu/en/references/references-map.php [accessed 31.05.15].

[3] Triogen. List of Triogen ORCs installed throughtout the world. 2015 [Online]. Available: http://www.triogen.nl/references/reference-overview [accessed 31.05.15].

[4] Elsevier. Scopus, abstract and citation database of peer-reviewed literature. 2015 [Online]. Literature Search URL, www.scopus.com., http://www.scopus.com/results/results.url?sort=plf-f&src=s&st1=organic+rankine+cycle+optimization&sid=0EE7B38754784CE1051A0F9D2A3C50EF.kqQeWtawXauCyC8ghhRGJg%3a50&sot=b&sdt=b&sl=49&s=TITLE-ABS-KEY%28organic+rankine+cycle+optimization%29&origin=searchbasic&editSaveSearch=&txGid=0EE7B38754784CE1051A0F9D2A3C50EF.kqQeWtawXauCyC8ghhRG Jg%3a5 [accessed 31.05.15].

[5] Dai Y, Wang J, Gao L. Parametric optimization and comparative study of Organic Rankine cycle (ORC) for low grade waste heat recovery. Energy Convers Manag Mar. 2009;50(3):576–82.

[6] Martelli E, Amaldi E. PGS-COM: a hybrid method for constrained non-smooth black-box optimization problems brief review, novel algorithm and comparative evaluation. Comput Chem Eng 2014;63(17):108–39.

[7] Papadopoulos AI, Stijepovic M, Linke P. "On the systematic design and selection of optimal working fluids for Organic Rankine Cycles. Appl Therm Eng May 2010;30(no. 6–7):760–9.

[8] Rashidi MM, Galanis N, Nazari F, Basiri Parsa a, Shamekhi L. Parametric analysis and optimization of regenerative Clausius and Organic Rankine cycles with two feedwater heaters using artificial bees colony and artificial neural network. Energy Sep. 2011;36(9):5728–40.

[9] S.A. Klein. Engineering equation Solver (EES). http://www.fchart.com/ees/ [accessed 31.05.15].

[10] Wang ZQ, Zhou NJ, Guo J, Wang XY. "Fluid selection and parametric optimization of organic Rankine cycle using low temperature waste heat. Energy Apr. 2012;40(1):107–15.

[11] Wang J, Yan Z, Wang M, Ma S, Dai Y. "Thermodynamic analysis and optimization of an (organic Rankine cycle) ORC using low grade heat source. Energy Jan. 2013;49:356–65.

[12] Conn a R, Gould N, Toint PL. A globally convergent Lagrangian barrier algorithm for optimization with general inequality constraints and simple bounds. Math Comput Jan. 1997;66(217):261–89.

[13] MathWorks. Global optimization Toolbox. http://www.mathworks.it/it/products/global-optimization/ [accessed 31.05.15].

[14] Wang J, Yan Z, Wang M, Li M, Dai Y. Multi-objective optimization of an organic Rankine cycle (ORC) for low grade waste heat recovery using evolutionary algorithm. Energy Convers Manag Jul. 2013;71:146–58.

[15] Deb K, Member A, Pratap A, Agarwal S, Meyarivan T. A fast and elitist multiobjective genetic algorithm. IEEE Trans Evol Comput 2002;6(2):182–97. Xi

[16] H, Li M-J, Xu C, He Y-L. Parametric optimization of regenerative organic Rankine cycle (ORC) for low grade waste heat recovery using genetic algorithm. Energy Sep. 2013;58:473–82.

[17] Pierobon L, Nguyen T, Larsen U, Haglind F, Elmegaard B. Multi-objective optimization of Organic Rankine cycles for waste heat recovery: application in an offshore platform. Energy Sep. 2013;58:538–49. http://dx.doi.org/10.1016/j.energy.2013.05.039.

[18] Lagarias JC, Reeds J a, Wright MH, Wright PE. Convergence properties of the Nelder–Mead simplex method in low dimensions. SIAM J Optim Jan. 1998;9(1):112–47.

[19] Andreasen JG, Larsen U, Knudsen T, Pierobon L, Haglind F. Selection and optimization of pure and mixed working fluids for low grade heat utilization using Organic Rankine Cycles. Energy 2014;73:204–13.

[20] Lecompte S, Huisseune H, van den Broek M, De Schampheleire S, De Paepe M. Part load based thermo-economic optimization of the Organic Rankine Cycle

(ORC) applied to a combined heat and power (CHP) system. Appl Energy Nov. 2013;111:871–81.
[21] Pierobon L, Casati E, Casella F, Haglind F, Colonna P. "Design methodology for flexible energy conversion systems accounting for dynamic performance. Energy Apr. 2014;68:667–79.
[22] Modelica Association. Modelica. https://www.modelica.org/ [accessed 31.05.15].
[23] Maraver D, Royo J, Lemort V, Quoilin S. Systematic optimization of subcritical and transcritical Organic Rankine Cycles (ORCs) constrained by technical parameters in multiple applications. Appl Energy Mar. 2014;117:11–29.
[24] Jones DR, Perttunen C, Stuckman B. Lipschitzian optimization without the Lipschitz constant. J Optim Theory Appl 1993;79(1):157–81.
[25] Walraven D, Laenen B, D'haeseleer W. Optimum configuration of shell-and-tube heat exchangers for the use in low-temperature Organic Rankine Cy-cles. Energy Convers Manag Jul. 2014;83:177–87.
[26] Biegler LT, Grossmann IE, Westerberg AW. Systematic methods of chemical pro-cess design. Upper Saddle River, New Jersey 07458: Prentice Hall PTR; 1997. p. 808.
[27] Buskens C, Wassel D. The ESA NLP solver WORHP. In: Modeling and optimization in space engineering. Springer; 2013. p. 85–110.
[28] Walraven D, Laenen B, D'haeseleer W. Economic system optimization of air-cooled Organic Rankine Cycles powered by low-temperature geothermal heat sources. Energy 2015;80:104–13.
[29] Larsen U, Sigthorsson O, Haglind F. A comparison of advanced heat recovery power cycles in a combined cycle for large ships. Energy Sep. 2014;74:260–8.
[30] Toffolo A, Lazzaretto A, Manente G, Paci M. A multi-criteria approach for the optimal selection of working fluid and design parameters in Organic Rankine Cycle systems. Appl Energy 2014;121:219–32.
[31] Toffolo A, Lazzaretto A, Morandin M. The HEATSEP method for the synthesis of thermal systems: an application to the S-Graz cycle. Energy 2010;35(2):976–81.
[32] MathWorks. Optimization Toolbox. http://it.mathworks.com/products/optimization/ [accessed 31.05.15].
[33] Manente G, Toffolo A, Lazzaretto A, Paci M. An Organic Rankine Cycle off-design model for the search of the optimal control strategy. Energy 2013;58:97–106.
[34] Astolfi M, Romano MC, Bombarda P, Macchi E. Binary ORC (Organic Rankine Cycles) power plants for the exploitation of medium–low temperature geothermal sources – part B: techno-economic optimization. Energy Mar. 2014;66:435–46.
[35] Macchi E, Perdichizzi A. Efficiency prediction for axial-flow turbines operating with nonconventional fluids. J Eng Gas Turbines Power 1981;103:712–24.
[36] Capra F, Martelli E. Numerical optimization of CHP Organic Rankine Cycles – part B: simultaneous design & part-load optimization. Energy 2015 [submitted for publication].
[37] Loo S, Jeppejan J. The handbook of biomass combustion and co-firing. London: Earthscan; 2008. p. 465.
[38] Martelli E, Nord L, Bolland O. Design criteria and optimization of heat recovery steam cycles for integrated reforming combined cycles with CO_2 capture. Appl Energy 2012;92(1):255–68.
[39] Bao J, Zhao L. A review of working fl uid and expander selections for organic Rankine cycle. Renew Sustain Energy Rev 2013;24:325–42.
[40] Hung TC, Shai TY, Wang SK. A review of Organic Rankine Cycles (ORCs) for the recovery of low-grade waste heat. Energy 1997;22:661–7.
[41] Hung TC, Wang SK, Kuo CH, Pei BS, Tsai KF. A study of organic working fluids on system efficiency of an ORC using low-grade energy sources. Energy 2010;35:1403–11.
[42] Invernizzi CM. Closed power cycles – thermodynamic fundamentals and applications. London: Springer-Verlag; 2013. p. 279.
[43] EPRI (Electric Power Research Institute). EPRI Report TR-102275. TAG – technical assessment guide (electric supply), vol. 1; 1993. Rev. 7.
[44] Lindroth P, Patriksson M. Pure categorical optimization – a global descent approach. Department of Mathematical Sciences, Division of Mathematics, Chalmers University of Technology, University of Gothenburg; 2011. p. 29.
[45] E.W. Lemmon, M.L. Huber, and M.O. Mclinden. NIST Reference Fluid Thermodynamic and Transport Properties — REFPROP. NIST Standard Reference Database 23, http://www.nist.gov/srd/nist23.cfm [accessed 31.05.15].
[46] Colonna P, Nannan NR, Guardone A. Multiparameter equations of state for siloxanes. Fluid Phase Equilib 2008;263:115–30.
[47] Lemmon EW, Span R. Short fundamental equations of state for 20 industrial fluids. J Chem Eng Data 2006;51:785–850.
[48] Dixon SL. Fluid mechanics, thermodynamics of Turbomachinery. 4th ed. Oxford: Butterworth-Heinemann; 1998. p. 353.
[49] Erhart T, Strzalka R, Eicker U, Infield D. Performance analysis of a biomass ORC poly-generation system. In: 2nd European Conference on Polygeneration, Terragona, Spain, 30 March–1 April 2011; 2011. p. 1–11.
[50] Erhart TG, Eicker U, Infield D. "Influence of condenser conditions on organic rankine cycle load characteristics. J Eng Gas Turbines Power Mar. 2013;135(4):042301.
[51] Ulrich DG, Vasudeva PT. Chemical engineering process design and economics. 2nd ed. New Hampshire (Durham): Process Publishing; 2004.
[52] Thermoflow. Thermoflex v. 24, " http://www.thermoflow.com/combinedcycle_TFX.html [accessed 31.05.15].
[53] Hu X, Eberhart R. Solving constrained nonlinear optimization problems with particle swarm optimization. In: Proceedings of the 6th world multi-conference on systematics, cybernetics and informatics, July 14–18, 2002, Orlando, USA; 2002. p. 203–6.
[54] Lewis RM, Shepherd A, Torczon V. Implementing generating set search methods for linearly constrained minimization. SIAM J Sci Comput Jan. 2007;29(6):2507–30.
[55] Andersson J. Multiobjective optimization in engineering design: application to fluid power systems. Sweden: Department of Mechanical Engineering, Linköpings Universitet; 2001, ISBN 91-7219-943-1 (Ph.D. thesis).
[56] Tańczuk M, Ulbrich R. "Implementation of a biomass-fired co-generation plant supplied with an ORC (Organic Rankine Cycle) as a heat source for small scale heat distribution system – a comparative analysis under Polish and German conditions. Energy Dec. 2013;62:132–41.